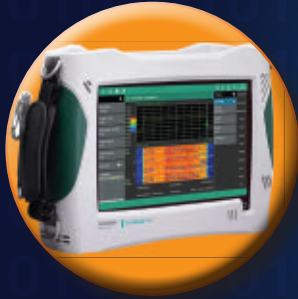


September/October 2023 | mwrf.com

# Microwaves & RF<sup>®</sup>



# WIRELESS T&M

*Ramps Up for the Future*

# PULSAR

MICROWAVE CORPORATION

## DC to 85 GHz

HIGH PERFORMANCE COMPONENTS



**Directional Couplers, to 60 GHz**  
Single and Dual  
High Power, to 2500 watts



**Power Dividers, to 70 GHz**  
2-32 Way



**Bias Tees, to 85 GHz**  
From 30 KHz



**Hybrids, to 40 GHz**  
90° & 180°

**CUSTOMIZATION AVAILABLE, QUOTES IN 24 HOURS.**  
[www.pulsarmicrowave.com](http://www.pulsarmicrowave.com)

48 Industrial West, Clifton, NJ 07012 | email: [sales@pulsarmicrowave.com](mailto:sales@pulsarmicrowave.com)  
Tel: 973-779-6262 • Fax: 973-779-2727

**RoHS Compliant**  
**ISO 9001:2008 Certified**  
60/40 Solder Also Available

# CONTENTS

September/October 2023 | VOLUME 62, ISSUE 5

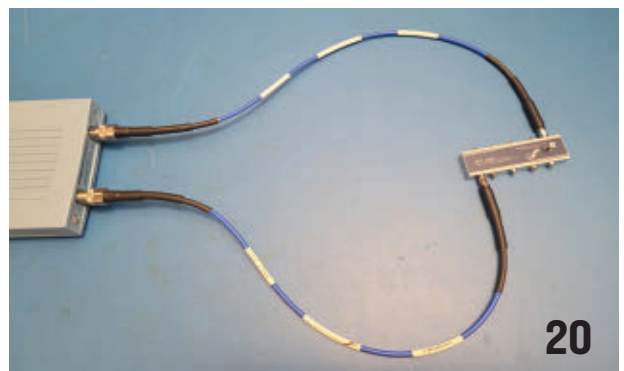
## FEATURES

- 14 Making the Software-Defined Vehicle a Reality
- 20 An Introduction to the VNA and Vector Network Analysis
- 24 **Cover Story:** State-of-the-Art Testers Chase Complex Wireless Signals
- 30 **Defense Electronics:** Phase-Noise Modeling, Simulation, and Propagation in Phase-Locked Loops (Part 2)

Cover credit: kraphix #1182341960 | iStock/Getty Images Plus

## DEPARTMENTS

- 4 From the Editor
- 5 Ad Index
- 6 Watch & Connect @ mwrf.com
- 8 News
- 12 Featured Products
- 35 New Products





DAVID MALINIAK, Senior Editor

# Non-Terrestrial Satellite Networks on the Ascent

The 3GPP's 2022 standards for non-terrestrial networks have spawned a boom in convergence of satellite communications and cellular networks.



130178724 © Dezzor | Dreamstime.com

**IN JUNE 2022**, the 3rd Generation Partnership Project (3GPP) published [standards](#) for integration of non-terrestrial networks (NTNs, or satellite networks) with terrestrial 5G networks. The goal of such integration is to use satellite constellations to deliver mobile services and network access to remote areas, and the hoped-for result is a new era of IoT/IIoT and mobile connectivity.

A recent [whitepaper](#) published by New York-based ABI Research digs into emerging trends and key players in the NTN mobile market. The satcom industry is seeing a profound impact from the opportunities afforded by the NTN-terrestrial network convergence. Operators like [Globalstar](#), [Intelsat](#), [OneWeb](#), [OQ Technology](#), [Sateliot](#), [SpaceX](#), [Viasat](#), and others are scrambling for collaborations with IoT solution providers such as eSAT Global, hiSky, Skylo Technologies, and Wyld Networks that will result in IoT services with ubiquitous connectivity.

Meanwhile, the giants in smartphones and mobile chipsets like [Apple](#), [Huawei](#), [MediaTek](#), [Motorola](#), [Qualcomm](#), and [ZTE](#) are all pushing forward with support for satellite communications by means of Narrowband-NTN, NTN unmodified, and, eventually, 5G New Radio-NTN.

All of this is helped along by smaller satellite form factors and greatly reduced launch costs. Satellite constellations in low Earth orbit lend themselves to low-latency, high-throughput network deployments, which in turn drives adoption of satcom services in the global telecommunications market. ABI Research foresees \$124.6 billion in annual satellite-services revenue by the end of this decade.

Some of the trends that will define the NTN mobile market include:

- **NTN as a mitigator of cellular network disconnectivity:** An analysis by Lynk shows that some 3 billion mobile users experience long periods of cellular outage every year. NTN connectivity can be the technology that fills in those gaps.
- **Emergency services will dominate early satellite-to-mobile opportunities:** In the short term, emergency services communications using NB-IoT and NTN unmodified devices will comprise most use cases. While terrestrial networks can fail during natural disasters, NTNs serve as a backstop to keep cellular coverage up and running for calls to first responders.
- **Enterprise opportunities are in business-critical applications in hard-to-reach areas:** NTN mobile will be important in remote operations for rural workers, transportation, utilities, oil and gas, mining, and logistics.

On top of that, look for opportunities in satellite IoT, especially in use cases of low complexity and data transmissions that are aperiodic. In these applications, energy saving is important. This means things like fleet management, condition-based monitoring, and asset tracking. Demand for satellite IoT services is being driven by the greater availability of LEO deployments, lower satellite launch costs, and CubeSat technology, which often can be built with off-the-shelf components and “piggybacked” onto other launch missions.

Read more articles in the [TechXchanges: IoT & Narrowband Communications](#) and [The Internet of Things \(IoT\)](#). ■

*David Maliniak*

[dmaliniak@endeavorb2b.com](mailto:dmaliniak@endeavorb2b.com)

## EDITORIAL ADVISORY BOARD



**DANIEL MONOPOLI**  
Chief Technology Officer, Wireless Telecom Group



**DONNA MOORE**  
CEO and chairwoman, LoRa Alliance



**TONY TESTA**  
Director-Marketing, Wireless Connectivity Business Unit, Qorvo



**SHERRY HESS**  
Product Marketing Group Director, Cadence



**NIZAR MESSAOUDI**  
Product Manager for Performance Network Analyzers, Keysight Technologies



**TONY MESSINA**  
Director of Design Engineering, Aerospace & Defense, Analog Devices Integrated Solutions



**DAVE DURBIN**  
Director of Engineering & Vice President for Quantic PMI (Planar Monolithics)



**GIORGIA ZUCHELLI**  
Product Manager, RF and Mixed-Signal, MathWorks

## AD INDEX

|                                     |     |
|-------------------------------------|-----|
| ACCEL-RF INSTRUMENTS CORP.....      | 7   |
| ANRITSU AMERICA SALES COMPANY ..... | 19  |
| AVTECH ELECTROSYSTEMS LTD.....      | 9   |
| CIAO WIRELESS, INC.....             | 11  |
| COILCRAFT, INC.....                 | 17  |
| MARKI MICROWAVE.....                | 23  |
| POLYFET RF DEVICES.....             | 29  |
| PULSAR MICROWAVE.....               | IFC |
| WEST BOND, INC. ....                | 27  |

### EDITORIAL

**Group Content Director:** Michelle Kopier  
mkopier@endeavorb2b.com

**Senior Content Editor:** Bill Wong  
bwong@endeavorb2b.com

**Senior Editor:** David Maliniak  
dmaliniak@endeavorb2b.com

**Managing Editor:** Roger Engelke  
rengelke@endeavorb2b.com

**Editor-at-Large:** Alix Paultre  
apaultre@endeavorb2b.com

**Senior Staff Writer:** James Morra  
jmorra@endeavorb2b.com

**Technical Editor:** Jack Browne  
jack.browne@citadeleng.com

### ART & PRODUCTION

**Group Design Director:** Anthony Vitolo

**Art Director:** Jocelyn Hartzog

**Production Manager:** Brenda Wiley

**Ad Services Manager:** Deanna O'Byrne

### AUDIENCE MARKETING

**User Marketing Manager:** Debbie Brady  
dbrady@endeavorb2b.com

**Article Reprints:**  
reprints@endeavorb2b.com

### LIST RENTAL

**Smartreach Client Services Manager:**  
Mary Ralicki, mralicki@endeavorb2b.com

### DIGITAL & MARKETING

**VP Digital & Data Innovation:** Ryan Malec

### SALES

**AL, AR, SOUTHERN CA, CO, FL, GA, HI, IA, ID, IL, IN, KS, KY, LA, MI, MN, MO, MS, MT, NC, ND, NE, OH, OK, SC, SD, TN, UT, VA, WI, WV, WY, CENTRAL CANADA:**  
Jamie Allen, jallen@endeavorb2b.com

**AZ, NM, TX:** Gregory Montgomery  
gmontgomery@endeavorb2b.com

Microwaves & RF Magazine ID Statement 2023:

**Microwaves & RF** ISSN 2162-1411 online, is published 6 times a year (January/February, March/April, May/June, July/August, September/October, November/December) by Endeavor Business Media, LLC, 1233 Janesville Ave., Fort Atkinson, WI 53538.

**POSTMASTER:** Send address changes to Microwaves & RF, PO Box 3257, Northbrook, IL 60065-3257. **SUBSCRIPTIONS:** Publisher reserves the right to reject non-qualified subscriptions. Subscription prices: U.S. \$68.75 per year; Canada/Mexico \$81.25 per year; All other countries \$93.75 per year. All subscriptions are payable in U.S. funds. Send subscription inquiries to Microwaves & RF, PO Box 3257, Northbrook, IL 60065-3257. Customer service can be reached toll-free at 877-382-9187 or at microwavesRF@meda.com for magazine subscription assistance or questions.

Printed in the USA. Copyright 2023 Endeavor Business Media, LLC. All rights reserved. No part of this publication may be reproduced or transmitted in any form or by any means, electronic or mechanical, including photocopies, recordings, or any information storage or retrieval system without permission from the publisher. Endeavor Business Media, LLC does not assume and hereby disclaims any liability to any person or company for any loss or damage caused by errors or omissions in the material herein, regardless of whether such errors result from negligence, accident, or any other cause whatsoever. The views and opinions in the articles herein are not to be taken as official expressions of the publishers, unless so stated. The publishers do not warrant either expressly or by implication, the factual accuracy of the articles herein, nor do they warrant any views or opinions by the authors of said articles.

**CT, DE, MA, MD, ME, NH, NJ, NY, PA, RI, VT, EASTERN CANADA:**

Elizabeth Eldridge  
eeldridge@endeavorb2b.com

**AK, NORTHERN CA, NV, OR, WA, WESTERN CANADA, AUSTRIA, BELGIUM, FRANCE, GERMANY, LUXEMBURG, NETHERLANDS, PORTUGAL, SCANDINAVIA, SPAIN, SWITZERLAND, UNITED KINGDOM:**

Stuart Bowen,  
sbowen@endeavorb2b.com

**ITALY:** Diego Casiraghi,  
diego@casiraghi-adv.com

**PAN-ASIA:** Helen Lai  
helen@twoway-com.com

**PAN-ASIA:** Charles Liu  
liu@twoway-com.com



### ENDEAVOR BUSINESS MEDIA, LLC

30 Burton Hills Blvd., Suite 185,  
Nashville, TN 37215 | 800-547-7377

**CEO:** Chris Ferrell

**President:** June Griffin

**CFO:** Mark Zadell

**COO:** Patrick Rains

**CRO:** Reggie Lawrence

**Chief Digital Officer:** Jacquie Niemiec

**Chief Administrative and Legal Officer:**  
Tracy Kane

**EVP, Design & Engineering Group:**  
Tracy Smith

### DESIGN & ENGINEERING GROUP

*Electronic Design, Machine Design,  
Microwaves & RF, Power & Motion,  
SourceESB, Source Today, 3DX*



### Video ▶ RF Transmitter Powers Battery-Free IoT Sensors

Batteries are the bane of IoT sensors, but they're typically a requirement because conventional energy-harvesting solutions like solar panels are often impractical. One solution is to provide power wirelessly. Energous' PowerBridge is designed to send RF energy over the air and to devices with matching chips from the company that can store the energy for use by the device.

[www.mwr.com/21273182](http://www.mwr.com/21273182)




### Video ▶ Solutions for Cellular Repeaters and Automotive Compensators

With Guerrilla RF, wireless design engineers find a reliable partner when it comes to MMICs for infrastructure applications. In addition to a quick overview of the company's portfolio, which includes amplifiers with and without bypass, RF power detectors, mixer/amplifier combos, RF switches, and digital step attenuators (DSAs), we were updated on some of the company's latest offerings by Guerrilla RF's Jim Ahne.

[www.mwr.com/21271957](http://www.mwr.com/21271957)

 [linkedin.com/groups/3848060/profile](https://www.linkedin.com/groups/3848060/profile)

 [www.facebook.com/microwavesrf](https://www.facebook.com/microwavesrf)

 [www.youtube.com/@engineeringtvEBM](https://www.youtube.com/@engineeringtvEBM)  [@MicrowavesRF](https://twitter.com/MicrowavesRF)



### Software-Defined Instrumentation Plus AI: A New Era in Test

The convergence of artificial-intelligence tools and flexible, software-defined instrumentation has brought the test and measurement industry to the brink of a technological revolution. AI-powered solutions coupled with FPGA-based instruments enable real-time optimization, making testing faster and more adaptable across industries.

[www.mwr.com/21274777](http://www.mwr.com/21274777)



### Avoiding Common Missteps in PCB Design: A Manufacturer's Insights

We explore seven common mistakes in PCB design, offering a unique perspective from the manufacturer's standpoint. Learn about the missteps that can significantly affect manufacturability and a PCB's performance and lifespan.

[www.mwr.com/21274534](http://www.mwr.com/21274534)



### New LoRaWAN Distance World Record Set at 1,300 km

The long-term LoRaWAN distance world record of 832 kilometers (517 miles) has been broken—it now stands at 1,336 kilometers, or 830 miles.

[www.mwr.com/21273819](http://www.mwr.com/21273819)



## **Modular Solutions for Flexible Reliability Testing**

### **Industry Applications**

*Compound Semiconductor R&D  
Commercial Wireless  
Military & Aerospace  
Alternative Energy  
Automotive  
Telecom  
Satcom  
Space*

### **Test Solutions**

*Device Characterization  
RF & DC Accelerated Life Testing  
Microwave/mm-Wave Test Fixtures  
High Voltage Switching Life Testing  
HTOL/HTRB/Burn-in Testing*



**Accel-RF**  
Instruments Corporation

4380 Viewridge Ave., Ste D  
San Diego, CA 92123  
858-278-2074  
info@accelrf.com  
www.accelrf.com



# Digitally Tunable Modular RF Blocks Empower Mil/Aero Systems

The SCi blocks family consists of RF SiPs, RF sticks, and open modules to meet the requirements of next-generation defense and aerospace systems.

**WHEN IT COMES TO THE** size, weight, and performance requirements of advanced aerospace and defense systems, the best is barely good enough, as there's no second prize on the battlefield. Addressing these constantly growing demands, Spectrum Control recently introduced SCi Blocks (called "sky blocks"), a family of next-generation, digitally enabled, plug-and-play RF blocks.

These open, modular, and digitally enabled products are offered in three tiers: RF systems-in-packages (RFSiPs), RF "sticks," and Sensor Open Systems Architecture (SOSA)-aligned OpenVPX modules. The ultra-miniature and high-performance wideband downconverters and upconverters provide the next level of SWaP-C for electronic warfare (EW), signal intelligence (SIGINT), and intelligence surveillance and reconnaissance (ISR) applications.

The company also unveiled an OpenVPX RF transceiver, which provides fidelity handling of RF signals with integral digital control and uses a minimal number of interconnects to expand design and usage options. Delivering total spectrum awareness from 20 MHz to 18 GHz, with up to 16 GHz of contiguous spectral coverage and 2 GHz of instantaneous bandwidth, the integrated digital gateway delivers a level of intelligence and connectivity previously unavailable in legacy RF components.

Using a simple four-wire interface for command and control along with health and temperature monitoring, the high-performance downconverter stick offers a gain of 25 dB and noise figure of 14 to 17 dB across the entire frequency range. Features include a 3rd-order intercept (IP3) of 25 dBm and single tone spurious of  $\geq 60$  dBc, along with IF calibration features for optimum spectral performance.

The upconverter stick provides a gain of 20 dB, with a noise figure of 25 dB across the frequency span, and an IP3 of 30 dBm, as well as a single tone spurious of  $\geq -55$  dBc at  $-10$ -dBm input and maximum gain. It offers independent user-controllable input and output gain control of 31.5 dB, in 0.5-dB increments. Provided in compact 13- x 2-cm packages drawing 8 and 10 W, respectively, both the downconverter and upconverter modules are available as a board-only solution or in a high-isolation, hermetically sealed, metal enclosure.

These wideband downconverter and upconverter sticks can be integrated into the SCi Block's 3U eight-channel OpenVPX transceiver module in any combination, supporting up to eight downconverter or eight upconverter channels. Fully SOSA-aligned, the modules also have a Modular Open Radio Frequency Architecture (MORA) device layer for configuration and control, plus an RF interface compliant to VITA 67.3. ■

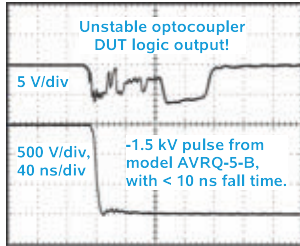


Images courtesy Spectrum Control



## Transient Immunity Testers

The Avtech AVRQ series of high-voltage, high-speed pulsers is ideal for testing the common-mode transient immunity (CMTI) of next-gen optocouplers, isolated gate drivers, and other semiconductors. GPIB, RS-232, Ethernet ports are standard.



- ♦ Kilovolt amplitudes ( $\pm 1$  kV,  $\pm 1.5$  kV,  $\pm 2$  kV)
- ♦ Transition times down to  $< 10$  ns, dV/dt rates up to 120 kV/us
- ♦ Daughterboards to handle a variety of DUT package styles



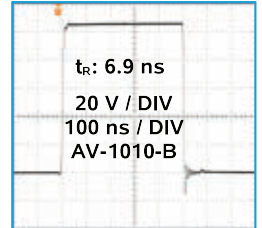
Nanosecond Electronics  
Since 1975

Pricing, manuals, datasheets and test results at:  
<http://www.avtechpulse.com/semiconductor>

## 30, 50 and 100 Volt Lab Pulsers



Avtech offers an extensive series of user-friendly  $\pm 30$ V,  $\pm 50$ , and  $\pm 100$  Volt general-purpose lab pulsers. In many applications, these can replace the discontinued Agilent 8114A or HP214. Higher-voltage models are also available.



- AV-1015-B:  $\pm 50$ V, 10 MHz, 20 ns - 10 ms, 10 ns rise
- AV-1010-B:  $\pm 100$ V, 1 MHz, 20 ns - 10 ms, 10 ns rise
- AV-1011B1-B:  $\pm 100$ V, 100 kHz, 100 ns - 1 ms, 2 ns rise
- AV-1011B3-B:  $\pm 30$ V, 100 kHz, 100 ns - 10 ms, 0.5 ns rise

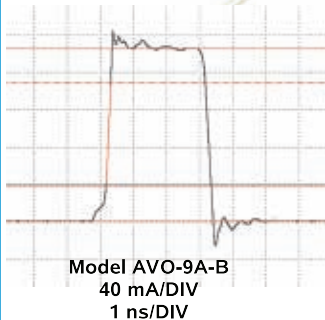
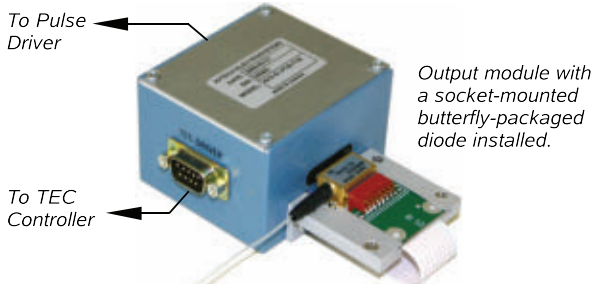
Includes switchable output impedance and double-pulse modes. Flexible triggering. GPIB / RS-232 / Ethernet.



Nanosecond Electronics  
Since 1975

Pricing, manuals, datasheets and test results at:  
<http://www.avtechpulse.com/general>

## Nanosecond Laser Diode Drivers With Butterfly Diode Sockets



Each of the 18 models in the Avtech **AVO-9 Series** of pulsed laser diode drivers includes a replaceable output module with an ultra-high-speed socket, suitable for use with sub-nanosecond pulses.

Models with maximum pulse currents of 0.2A to  $>10$ A are available, with pulse widths from 400 ps to 1 us.

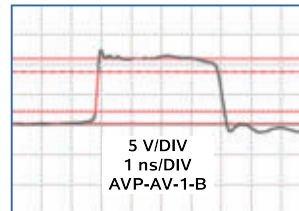
GPIB, RS-232, and Ethernet control available.



Nanosecond Electronics  
Since 1975

Pricing, manuals, datasheets and test results at:  
<http://www.avtechpulse.com/laser>

## High Output, Low Risetime Pulsers



Nanosecond and faster pulsers covering a wide range of amplitudes!

GPIB / RS-232 / Ethernet standard on "B" models.

Standard and customized models available.

| Ampl  | trISE  | Max. PRF | Model        |
|-------|--------|----------|--------------|
| 5 V   | 80 ps  | 1 MHz    | AVP-AV-1S-C  |
| 10 V  | 120 ps | 1 MHz    | AVP-AV-1-B   |
| 20 V  | 120 ps | 1 MHz    | AVP-AV-HV2-B |
| 20 V  | 200 ps | 10 MHz   | AVMR-2D-B    |
| 40 V  | 150 ps | 1 MHz    | AVP-AV-HV3-B |
| 50 V  | 500 ps | 1 MHz    | AVR-E5-B     |
| 100 V | 500 ps | 100 kHz  | AVR-E3-B     |
| 100 V | 300 ps | 20 kHz   | AVI-V-HV2A-B |
| 200 V | 1 ns   | 50 kHz   | AVIR-1-B     |
| 200 V | 2 ns   | 20 kHz   | AVIR-4D-B    |
| 400 V | 2.5 ns | 2 kHz    | AVL-5-B-TR   |



Nanosecond Electronics  
Since 1975

Pricing, manuals, datasheets and test results at:  
<http://www.avtechpulse.com/laser>

## 3D Coil Receiver Antenna for VR/AR Claimed as Smallest Available

### PREMO RECENTLY LAUNCHED

the 3DCC03 series, presented as the smallest 3D coil receiver antenna to date. Coming in at 60% the size of its predecessor, the antenna is designed to address miniaturization of electromagnetic (EM) motion-tracking sensors and other tracking applications.

The 3DCC03 series has a novel design incorporating the receivers for three axes in a single core, creating an extremely small solution measuring  $4.2 \times 3.2 \times 3.5$  mm. The antennas offer excellent isotropy, with the same sensitivity in X, Y, and Z axes. They have a working frequency of 20 kHz, provide connectivity via six gold-finished pads, and meet MIL-STD 202, with an operating temperature range from  $-40$  to  $+85^\circ\text{C}$ .



With a small size to ease integration into space-challenged applications having limited space, such as VR/AR headsets, wearable devices, and industrial automation equipment, the antenna enables simultaneous tracking of multiple small elements, such as fingers, pens, or small wearable devices. Compared to optical, inertial, and mechanical tracking sensors, EM sensors offer freedom of movement: They don't require line of sight, don't drift over time, and have lower latency for more responsive tracking data. They also perform well inside or through the human body due to its large wavelength. ■



**CONCRETE IS A NECESSARY** ingredient of modern highway infrastructure, but not quite so much of it may be required. A sensor developed at Purdue University and embedded directly into a concrete pour may enable concrete to “talk” about its condition and when it needs repairs. It may also improve the sustainability of roads using concrete and lead to less concrete for the road infrastructure. Because making concrete contributes so much to the world's carbon gas footprint, the sensor could significantly reduce the carbon footprint, too.

Luna Lu, the Reilly Professor and acting head of Purdue's Lyles School of Civil Engineering, has been leading the development of the sensor since 2017. The sensor provides more precise data about the concrete's condition than possible with current measurement methods. Traffic jams during road repairs consume 4 billion hours and 3 billion gallons of gas per year. This sensor could help curb those numbers.

According to the U.S. Federal Highway Administration (FHA), concrete pavement forms less than 2% of U. S. roads but about 20% of the highway system, and the material is difficult to repair. Many states, including California and Texas, have agreed to implement the sensors as part of an FHA-pooled fund.

### REBEL Sensors

The sensors will also be marketed as the REBEL Concrete Strength Sensing System (see image above), produced by WaveLogix, a company founded by Lu in 2021. The company licenses the technology from the Purdue Research Foundation Office of Technology Commercialization, which has applied for patent protection in intellectual property (IP).

The innovative sensor may replace testing methods that have served as the industry's standards since the early 1900s. Those techniques involve analyzing large samples of concrete in a laboratory or on-site facility. With that data, estimates are made of the strength of a particular concrete mix after it's been poured and left to mature at a construction site. Discrepancies between laboratory and outdoor conditions can lead to inaccurate estimates of the concrete's strength.

Lu believes that the new method, when used with artificial intelligence (AI), could reduce the amount of cement used in concrete mixes by 20% to 25%. The approach would simultaneously make pavement more durable and less expensive.

“I feel a strong sense of responsibility to make an impact on our infrastructure through developing new types of technology,” said Lu. “In the field of civil engineering, if we don't make an impact on the world, there won't be a world to worry about.”

The sensor uses wireless technology via cellular telephone networks to communicate data from the road. ■

# RF Amplifiers and Sub-Assemblies for Every Application

Delivery from Stock to 2 Weeks ARO from the catalog or built to your specifications!

- Competitive Pricing & Fast Delivery
- Military Reliability & Qualification
- Various Options: Temperature Compensation, Input Limiter Protection, Detectors/TTL & More
- Unconditionally Stable (100% tested)

ISO 9001:2000  
and AS9100B  
CERTIFIED



## OCTAVE BAND LOW NOISE AMPLIFIERS

| Model No.   | Freq (GHz) | Gain (dB) MIN | Noise Figure (dB) | Power-out @ P1-dB | 3rd Order ICP | VSWR  |
|-------------|------------|---------------|-------------------|-------------------|---------------|-------|
| CA01-2110   | 0.5-1.0    | 28            | 1.0 MAX, 0.7 TYP  | +10 MIN           | +20 dBm       | 2.0:1 |
| CA12-2110   | 1.0-2.0    | 30            | 1.0 MAX, 0.7 TYP  | +10 MIN           | +20 dBm       | 2.0:1 |
| CA24-2111   | 2.0-4.0    | 29            | 1.1 MAX, 0.95 TYP | +10 MIN           | +20 dBm       | 2.0:1 |
| CA48-2111   | 4.0-8.0    | 29            | 1.3 MAX, 1.0 TYP  | +10 MIN           | +20 dBm       | 2.0:1 |
| CA812-3111  | 8.0-12.0   | 27            | 1.6 MAX, 1.4 TYP  | +10 MIN           | +20 dBm       | 2.0:1 |
| CA1218-4111 | 12.0-18.0  | 25            | 1.9 MAX, 1.7 TYP  | +10 MIN           | +20 dBm       | 2.0:1 |
| CA1826-2110 | 18.0-26.5  | 32            | 3.0 MAX, 2.5 TYP  | +10 MIN           | +20 dBm       | 2.0:1 |

## NARROW BAND LOW NOISE AND MEDIUM POWER AMPLIFIERS

| Model No.   | Freq (GHz)   | Gain (dB) MIN | Noise Figure (dB) | Power-out @ P1-dB | 3rd Order ICP | VSWR  |
|-------------|--------------|---------------|-------------------|-------------------|---------------|-------|
| CA01-2111   | 0.4 - 0.5    | 28            | 0.6 MAX, 0.4 TYP  | +10 MIN           | +20 dBm       | 2.0:1 |
| CA01-2113   | 0.8 - 1.0    | 28            | 0.6 MAX, 0.4 TYP  | +10 MIN           | +20 dBm       | 2.0:1 |
| CA12-3117   | 1.2 - 1.6    | 25            | 0.6 MAX, 0.4 TYP  | +10 MIN           | +20 dBm       | 2.0:1 |
| CA23-3111   | 2.2 - 2.4    | 30            | 0.6 MAX, 0.45 TYP | +10 MIN           | +20 dBm       | 2.0:1 |
| CA23-3116   | 2.7 - 2.9    | 29            | 0.7 MAX, 0.5 TYP  | +10 MIN           | +20 dBm       | 2.0:1 |
| CA34-2110   | 3.7 - 4.2    | 28            | 1.0 MAX, 0.5 TYP  | +10 MIN           | +20 dBm       | 2.0:1 |
| CA56-3110   | 5.4 - 5.9    | 40            | 1.0 MAX, 0.5 TYP  | +10 MIN           | +20 dBm       | 2.0:1 |
| CA78-4110   | 7.25 - 7.75  | 32            | 1.2 MAX, 1.0 TYP  | +10 MIN           | +20 dBm       | 2.0:1 |
| CA910-3110  | 9.0 - 10.6   | 25            | 1.4 MAX, 1.2 TYP  | +10 MIN           | +20 dBm       | 2.0:1 |
| CA1315-3110 | 13.75 - 15.4 | 25            | 1.6 MAX, 1.4 TYP  | +10 MIN           | +20 dBm       | 2.0:1 |
| CA12-3114   | 1.35 - 1.85  | 30            | 4.0 MAX, 3.0 TYP  | +33 MIN           | +41 dBm       | 2.0:1 |
| CA34-6116   | 3.1 - 3.5    | 40            | 4.5 MAX, 3.5 TYP  | +35 MIN           | +43 dBm       | 2.0:1 |
| CA56-5114   | 5.9 - 6.4    | 30            | 5.0 MAX, 4.0 TYP  | +30 MIN           | +40 dBm       | 2.0:1 |
| CA812-6115  | 8.0 - 12.0   | 30            | 4.5 MAX, 3.5 TYP  | +30 MIN           | +40 dBm       | 2.0:1 |
| CA812-6116  | 8.0 - 12.0   | 30            | 5.0 MAX, 4.0 TYP  | +33 MIN           | +41 dBm       | 2.0:1 |
| CA1213-7110 | 12.2 - 13.25 | 28            | 6.0 MAX, 5.5 TYP  | +33 MIN           | +42 dBm       | 2.0:1 |
| CA1415-7110 | 14.0 - 15.0  | 30            | 5.0 MAX, 4.0 TYP  | +30 MIN           | +40 dBm       | 2.0:1 |
| CA1722-4110 | 17.0 - 22.0  | 25            | 3.5 MAX, 2.8 TYP  | +21 MIN           | +31 dBm       | 2.0:1 |

## ULTRA-BROADBAND & MULTI-OCTAVE BAND AMPLIFIERS

| Model No.   | Freq (GHz) | Gain (dB) MIN | Noise Figure (dB) | Power-out @ P1-dB | 3rd Order ICP | VSWR  |
|-------------|------------|---------------|-------------------|-------------------|---------------|-------|
| CA0102-3111 | 0.1-2.0    | 28            | 1.6 Max, 1.2 TYP  | +10 MIN           | +20 dBm       | 2.0:1 |
| CA0106-3111 | 0.1-6.0    | 28            | 1.9 Max, 1.5 TYP  | +10 MIN           | +20 dBm       | 2.0:1 |
| CA0108-3110 | 0.1-8.0    | 26            | 2.2 Max, 1.8 TYP  | +10 MIN           | +20 dBm       | 2.0:1 |
| CA0108-4112 | 0.1-8.0    | 32            | 3.0 MAX, 1.8 TYP  | +22 MIN           | +32 dBm       | 2.0:1 |
| CA02-3112   | 0.5-2.0    | 36            | 4.5 MAX, 2.5 TYP  | +30 MIN           | +40 dBm       | 2.0:1 |
| CA26-3110   | 2.0-6.0    | 26            | 2.0 MAX, 1.5 TYP  | +10 MIN           | +20 dBm       | 2.0:1 |
| CA26-4114   | 2.0-6.0    | 22            | 5.0 MAX, 3.5 TYP  | +30 MIN           | +40 dBm       | 2.0:1 |
| CA618-4112  | 6.0-18.0   | 25            | 5.0 MAX, 3.5 TYP  | +23 MIN           | +33 dBm       | 2.0:1 |
| CA618-6114  | 6.0-18.0   | 35            | 5.0 MAX, 3.5 TYP  | +30 MIN           | +40 dBm       | 2.0:1 |
| CA218-4116  | 2.0-18.0   | 30            | 3.5 MAX, 2.8 TYP  | +10 MIN           | +20 dBm       | 2.0:1 |
| CA218-4110  | 2.0-18.0   | 30            | 5.0 MAX, 3.5 TYP  | +20 MIN           | +30 dBm       | 2.0:1 |
| CA218-4112  | 2.0-18.0   | 29            | 5.0 MAX, 3.5 TYP  | +24 MIN           | +34 dBm       | 2.0:1 |

## LIMITING AMPLIFIERS

| Model No.   | Freq (GHz) | Input Dynamic Range | Output Power Range Psat | Power Flatness dB | VSWR  |
|-------------|------------|---------------------|-------------------------|-------------------|-------|
| CLA24-4001  | 2.0 - 4.0  | -28 to +10 dBm      | +7 to +11 dBm           | +/- 1.5 MAX       | 2.0:1 |
| CLA26-8001  | 2.0 - 6.0  | -50 to +20 dBm      | +14 to +18 dBm          | +/- 1.5 MAX       | 2.0:1 |
| CLA712-5001 | 7.0 - 12.4 | -21 to +10 dBm      | +14 to +19 dBm          | +/- 1.5 MAX       | 2.0:1 |
| CLA618-1201 | 6.0 - 18.0 | -50 to +20 dBm      | +14 to +19 dBm          | +/- 1.5 MAX       | 2.0:1 |

## AMPLIFIERS WITH INTEGRATED GAIN ATTENUATION

| Model No.    | Freq (GHz)  | Gain (dB) MIN | Noise Figure (dB) | Power-out @ P1-dB | Gain Attenuation Range | VSWR   |
|--------------|-------------|---------------|-------------------|-------------------|------------------------|--------|
| CA001-2511A  | 0.025-0.150 | 21            | 5.0 MAX, 3.5 TYP  | +12 MIN           | 30 dB MIN              | 2.0:1  |
| CA05-3110A   | 0.5-5.5     | 23            | 2.5 MAX, 1.5 TYP  | +18 MIN           | 20 dB MIN              | 2.0:1  |
| CA56-3110A   | 5.85-6.425  | 28            | 2.5 MAX, 1.5 TYP  | +16 MIN           | 22 dB MIN              | 1.8:1  |
| CA612-4110A  | 6.0-12.0    | 24            | 2.5 MAX, 1.5 TYP  | +12 MIN           | 15 dB MIN              | 1.9:1  |
| CA1315-4110A | 13.75-15.4  | 25            | 2.2 MAX, 1.6 TYP  | +16 MIN           | 20 dB MIN              | 1.8:1  |
| CA1518-4110A | 15.0-18.0   | 30            | 3.0 MAX, 2.0 TYP  | +18 MIN           | 20 dB MIN              | 1.85:1 |

## LOW FREQUENCY AMPLIFIERS

| Model No.  | Freq (GHz) | Gain (dB) MIN | Noise Figure (dB) | Power-out @ P1-dB | 3rd Order ICP | VSWR  |
|------------|------------|---------------|-------------------|-------------------|---------------|-------|
| CA001-2110 | 0.01-0.10  | 18            | 4.0 MAX, 2.2 TYP  | +10 MIN           | +20 dBm       | 2.0:1 |
| CA001-2211 | 0.04-0.15  | 24            | 3.5 MAX, 2.2 TYP  | +13 MIN           | +23 dBm       | 2.0:1 |
| CA001-2215 | 0.04-0.15  | 23            | 4.0 MAX, 2.2 TYP  | +23 MIN           | +33 dBm       | 2.0:1 |
| CA001-3113 | 0.01-1.0   | 28            | 4.0 MAX, 2.8 TYP  | +17 MIN           | +27 dBm       | 2.0:1 |
| CA002-3114 | 0.01-2.0   | 27            | 4.0 MAX, 2.8 TYP  | +20 MIN           | +30 dBm       | 2.0:1 |
| CA003-3116 | 0.01-3.0   | 18            | 4.0 MAX, 2.8 TYP  | +25 MIN           | +35 dBm       | 2.0:1 |
| CA004-3112 | 0.01-4.0   | 32            | 4.0 MAX, 2.8 TYP  | +15 MIN           | +25 dBm       | 2.0:1 |

CIAO Wireless can easily modify any of its standard models to meet your "exact" requirements at the Catalog Pricing.

Visit our web site at [www.ciaowireless.com](http://www.ciaowireless.com) for our complete product offering.



Ciao Wireless, Inc. 4000 Via Pescador, Camarillo, CA 93012

Tel (805) 389-3224 Fax (805) 389-3629 sales@ciaowireless.com

# RTL Design Tool Brings Gains in Productivity, Quality of Results

## The Overview

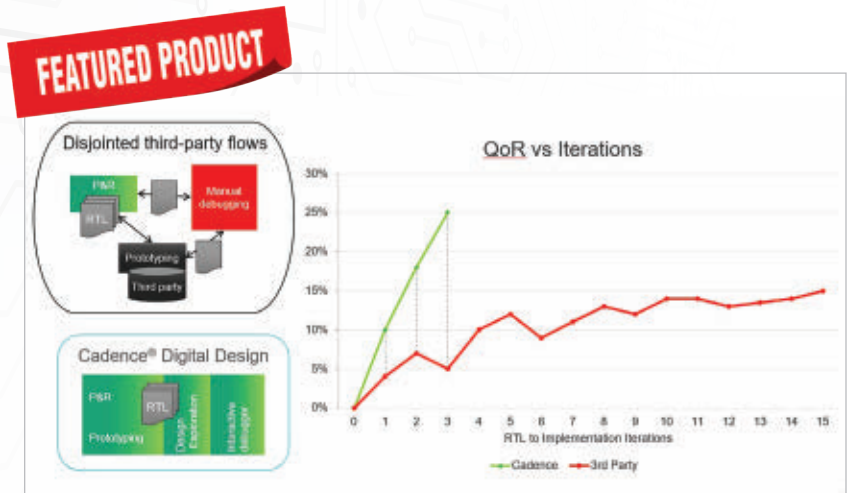
In its new Joules RTL Design Studio tool, Cadence Design Systems aims to provide users with information that will lead to a speedier register-transfer-level (RTL) design and implementation process. Through a single, unified cockpit, it affords front-end designers access to digital design analysis and debugging capabilities, from which they can attain a fully optimized RTL design before handing it off to implementation.

Joules RTL Design Studio also enables users to leverage generative AI for RTL design exploration and big-data analytics with the company's expansive AI portfolio. Users can get fast, accurate physical estimates, unlocking up to 5X productivity and up to 25% quality-of-results (QoR) improvements in the RTL.

## Who Needs It & Why?

For RTL designers, the sheer size and complexity of today's SoC designs means they need earlier—and deeper—visibility into physical design. If the RTL code that's handed off to implementation isn't fully optimized, the RTL designer runs the risk of handing off code that will yield low-quality netlists. The physical implementation process can only hope to attain modest improvement to those netlists.

Thus, it behooves the front-end designer to avoid kneecapping implementation. Joules RTL Design Studio accomplishes just that by shedding light onto critical physical aspects of the RTL code: power, performance, area, and congestion (PPAC). Armed with that insight, the RTL designer can then resolve a large portion of physical implementation challenges posed by their formative code, and by doing so, reduce the number of iterations between RTL design and physical implementation.



Cadence Design Systems

## Under the Hood

Joules RTL Design Studio brings a host of productivity-enhancing features and benefits. For one, it offers an intelligent RTL debugging assistant system, which is what delivers those critical early PPAC metrics as well as actionable debugging information throughout the design cycle—logical, physical, and production implementation. This enables exploration of “what-if” scenarios and potential resolutions to minimize iterations and improve design outcomes.

The tool is based on proven engines, as it shares the same trusted engines as Cadence's Innovus Implementation System, Genus Synthesis Solution, and Joules RTL Power Solution. Thus, users may access all analysis and design exploration features from a single GUI for optimal QoR.

Joules RTL Design Studio also provides powerful AI integrations, such as integration with Cadence's generative-AI solution, Cadence Cerebrus Intelligent Chip Explorer, to explore design space scenarios, such as floorplan optimization and frequency-vs.-voltage tradeoffs.

In addition, the Cadence Joint Enterprise Data and AI (JedAI) Platform allows for trend and insight analysis across different versions of the RTL or across previous project generations. There's also integration with lint checkers, so that users can run such tools incrementally to rule out data and setup issues up-front, reducing errors and time to completion.

Finally, the tool's unified cockpit provides RTL designers with an efficient, user-friendly experience, offering physical design feedback, localization and categorization of violations, bottleneck analysis, and cross-probing between RTL, schematic, and layout.

# 5G RedCap Release 17 Connectivity Successfully Verified

## The Overview

Rohde & Schwarz and MediaTek successfully verified MediaTek's 5G RedCap (reduced capability) test platform, as defined in 3GPP Release 17. Enabling an expanded range of 5G standalone devices, the solution is based on Rohde & Schwarz's CMX500 OBT wireless communications tester, which was tailored to support RedCap and other Release 17 features. The successful verification of its 5G RedCap test platform with the R&S CMX500 signaling tester gives MediaTek the green light to test, measure, and verify its final products with full confidence.

## Who Needs It & Why?

This solution will benefit anyone involved in wireless device development, as 5G RedCap introduces true mid-tier, enhanced machine-type communication (eMTC) to the 5G ecosystem. It will enable designers to launch advanced devices that expand and enhance the capability and complexity of legacy low-speed narrow-band IoT solutions with an optimized design for mid-tier use cases.

5G RedCap modems are less complex, use less spectrum bandwidth, consume less power, and work only in standalone (SA) mode, in contrast to 5G modems designed for eMBB use cases.

Christoph Pointner, Senior Vice President of Mobile Radio Testers at Rohde & Schwarz, said, "I am really honored that our R&S CMX500 will help the industry advance 5G and address new device types that support 5G RedCap in early R&D stages. We are committed to our close and long-standing partnership with MediaTek."

Dr. Ho-Chi Hwang, General Manager of Wireless Communication System and Partnerships at MediaTek added, "Continuing our close collaboration with Rohde & Schwarz has enabled MediaTek to verify an important milestone towards the next era of 5G. MediaTek will bring the new capabilities of 5G RedCap into our next-gen product lines."

## Under the Hood

Rohde & Schwarz optimized the R&S CMX500 OBT for IoT testing so that



Rohde & Schwarz

MediaTek could verify the various RedCap aspects defined in 3GPP 5G Rel. 17 for network access restrictions, bandwidth parts (BWP), bandwidth part switching, power saving, and other RedCap-specific protocol signaling procedures.

With a one-box tester configuration, the tester supports all relevant 5G frequencies up to 8 GHz via the R&S CMSquares web-based user interface. Suitable for all 5G mobile devices and chipsets, the CMX500-based signaling test solution supports all 5G NR network deployment configurations and frequency ranges. The R&S CMX500 OBT lite offers a cost-effective compact hardware configuration.

# First CTIA MIMO OTA Dynamic Channel Model Validation Solution Arrives



Keysight Technologies

## The Overview

Keysight Technologies, along with China Telecommunication Technology Labs (CTTL), released what is presented as the first MIMO over-the-air (OTA) dynamic channel model test and user-equipment (UE) performance validation system. Based on CTIA requirements for the 5G

New Radio (NR) FR1 frequency band, the solution benchmarks the performance of equipment from different manufacturers and chipset vendors.

UE can suffer from performance degradation during real-world use as a result of various propagation channel effects, which are addressed by optimizing UE hardware and software design. To do this and validate them under real-world conditions, designers need consistent, reliable, and repeatable digital twins emulating real-world channel effects.

## Who Needs It & Why?

Design engineers are consistently looking for new 5G dynamic MIMO test solutions to further expand their ability to

serve a wide range of customers. Using this solution, engineers can provide comprehensive services for research, development, testing, and certification across the entire industry. With this test system for MIMO OTA plus dynamic channel model validation, the industry can continue to drive the development of standards in CTIA.

## Under the Hood

Keysight and CTTL collaborated to create the solution by integrating the CTIA-compliant MIMO OTA test system with a dynamic channel model validation test. The new validation tool leverages Keysight's OTA Emulation Solutions for emulating real-world environments to perform OTA testing for UE with multiple antennas.



Photos courtesy NXP

# Making the Software-Defined Vehicle a Reality

Next-generation vehicles will be defined by software, not hardware, with cloud software concepts like containers delivering an agile approach to swapping out and updating software services.

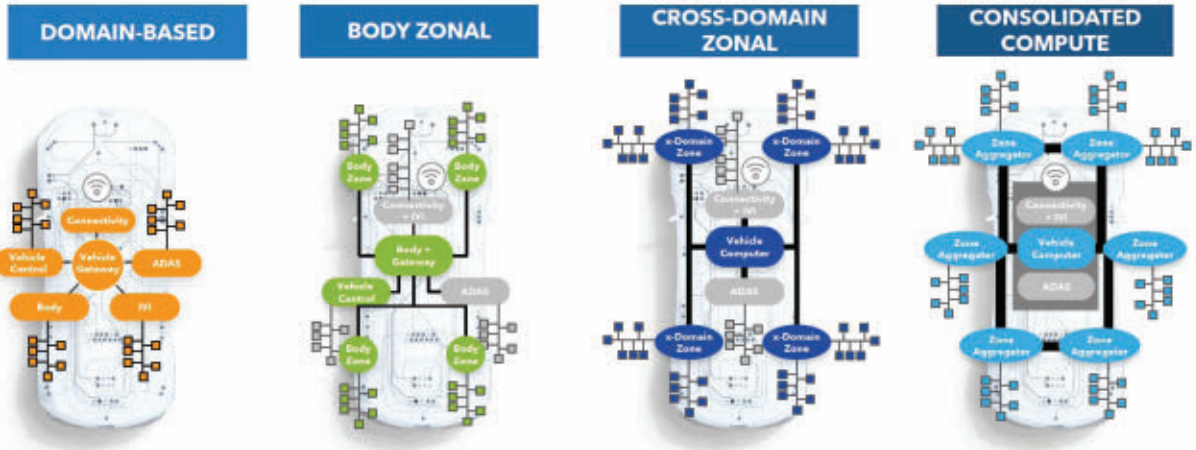
*By Thomas Brown, Solution Architect for Automotive Processing, NXP Semiconductors*

*Brian Carlson, Director of Global Product and Solutions Marketing, NXP Semiconductors*

**T**raditionally, vehicle original equipment manufacturers (OEMs) have sourced the needed boxes from their best suppliers, plugged them together, and—voilà—they produced a vehicle packed with technology that was popular with consumers from five years earlier.

There was never an option to upgrade any hardware, even though it was available on other vehicles from the same platform. This is due to the complexity of today's automotive supply chain, coupled with the cost and effort of integration, validation, and regulatory certification.

Nor could you update the software to take advantage of a new capability. In a best-case scenario, a software update would reluctantly be offered to resolve a minor issue. But things are changing with the [advent of the software-defined vehicle \(SDV\)](#).



1. Automotive manufacturers are moving toward domain and zonal architectures and away from a disparate array of ECUs.

The dream is to offer additional features to vehicles after they roll out to the driver on the road, enabling them to customize their cars, almost like they update their smartphones. And the driver may not even be the owner. Instead, following the trend of shared mobility, features and capabilities will follow the driver to the vehicle they use.

Vehicle electrical/electronic (E/E) architectures are changing dramatically to achieve this flexibility. **Domain and zonal architectures** (Fig. 1) mean that each hardware box integrated into the platform will be networked. This allows for data exchange across high-speed, time-sensitive Ethernet networks and collaboration between processors over PCIe.

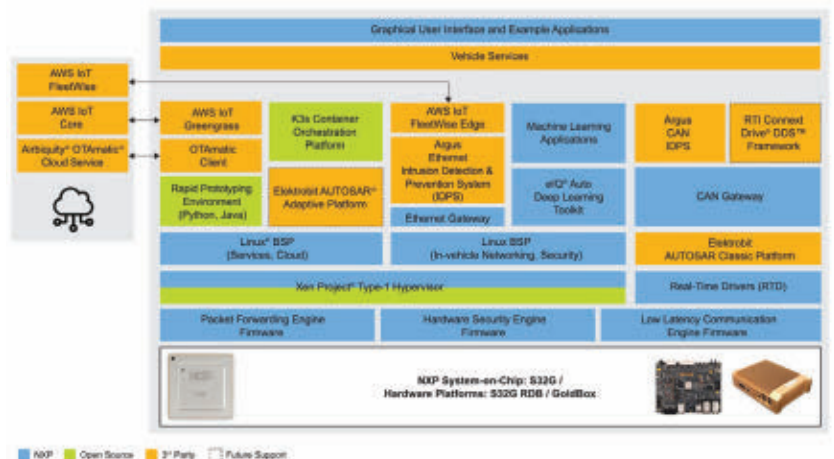
At the core of this new architecture is a vehicle computer coordinating functionality within the vehicle and interfacing with cloud services. Furthermore, functions may even be split across electronic control units (ECUs) so that, when manufactured, the hardware may not be programmed to execute a specific function. Instead, that decision will be made when the software is installed during vehicle manufacture, spreading it across the most appropriate resources.

**virtualization** and containerization have made software-as-a-service (SaaS) robust under extreme loading, cyberattacks, and during software updates. Virtualization uses a hypervisor to enable several operating systems (OSs) to run on a single server. Memory, storage, and networking are then shared across the OSs. However, virtualized OSs are slow to start when more resources are needed.

Containerization uses a single OS that provides separate user spaces (containers) for the applications it executes. Should one app go wrong or need updating, the others continue, unaffected by what's happening elsewhere.

In addition, if a container is operating at its limit, a replica can be quickly started to share the load, allowing for dynamic or “elastic” orchestration. Key technologies in this space are Kubernetes for operating containerized applications (Fig. 2) and Docker for creating containerized applications. But other, lighter-weight solutions are emerging that fit the needs of automotive systems more appropriately.

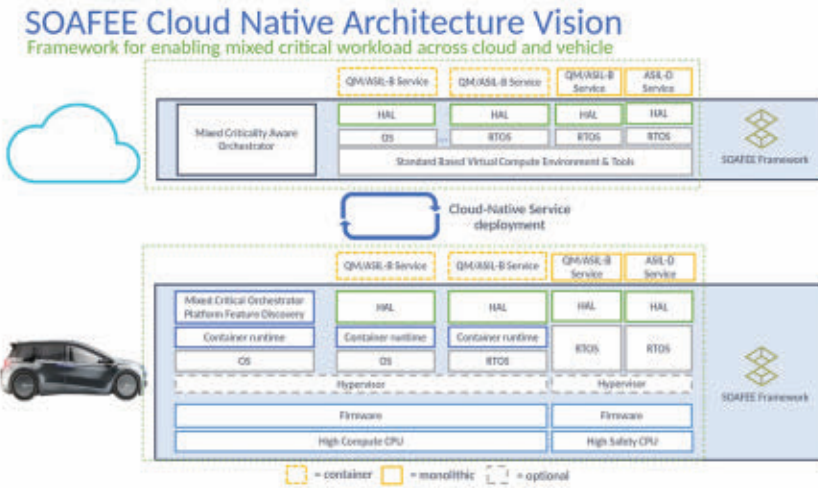
For automotive, K3s<sup>1</sup> is a highly available version of Kubernetes for resource-constrained hardware that supports Arm processors. Coupled with today's continuous integration/continuous deployment (CI/CD) software development process-



## Learning from the Cloud

The automotive industry is looking to the cloud for inspiration in making this happen inside the vehicle. There,

2. GoldVIP utilizes Kubernetes K3s for container orchestration. Two separate AWS services manage edge runtime and cloud services, with OTA updates handled by the OTAmatic client.



3. SOAFEE takes a cloud-native approach to automotive software development and has significant support from automotive industry heavyweights. (Credit: SOAFEE)

es and over-the-air (OTA) updates, the puzzle pieces are in place to support the SDV vision.

**Automotive Industry is Changing**

Recognizing that implementing such change is a task for a community, not just individuals, representatives from the semiconductor industry, cloud computing, automakers, and other suppliers have formed the Scalable Open Architecture for Embedded Edge (SOAFEE) project.<sup>2</sup> This industry-led collaboration includes companies such as Arm, AWS, Bosch, CARIAD, Continental, Red Hat, SUSE, and Woven by Toyota (Fig. 3).

The initiative encompasses not only software for vehicle hardware but also for the cloud with a cloud-native software development approach. Cloud services are used to create a CI/CD pipeline for building, containerizing, validating, and deploying software that works both in the cloud and on embedded hardware.

Naturally, the project covers security, supports real-time needs, and provides support for functional safety through mixed-criticality awareness. Thus, comfort features can be deployed or updated without impacting services related to safety-critical capabilities.

If vehicle feature differentiation is to come through software, the higher-level application software is meant to define differentiation, not the lower-level software. There are other similar approaches.

One such approach is Vehicle OS from Vector. Its runtime environment is known as Base Layer, which can be adapted for microcontrollers, microprocessors, or a cloud-based backend. Delivering this environment is Software Factory, which automates the development workflow, integration of low-level software, middle-

ware, and apps, with distribution to the vehicle or backend.

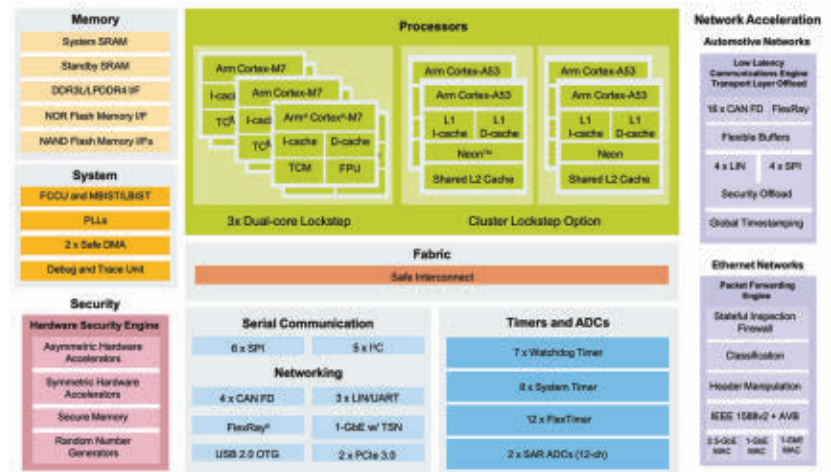
TTTech Auto also sees a future for an open standard Car.OS,<sup>3</sup> noting that most infotainment software is built on a common software stack. Such an approach also supports the “develop once, deploy many times” ethos already highlighted.

**Hardware for the Software**

While cloud applications can be very robust and reliable, this is achieved through brute-force computing power and massive, elastic redundancy on an x86 hardware platform that’s common across the industry.

To replicate it in the vehicle, a new generation of processors is needed that fulfill these capabilities while also delivering high-speed networking, determinism, and functional safety. And, due to the increased attack surface resulting from these mobile networked devices, a carefully constructed approach to cybersecurity in both software and hardware is needed.

A new generation of vehicle network processors is at the forefront of enabling the SDV revolution. One example is the NXP S32G3 family, which builds on the capabilities of the previous generation of automotive compute silicon (Fig. 4). The design tackles the three main



4. The S32G3 targets ASIL D applications in new SDV E/E architectures such as safety processors for autonomous driving, central compute nodes, and service-oriented gateways.



# Find the Right Part Faster



Designed by Engineers for Engineers, our **MAGPro™** RF Inductor and Choke Finder helps you find the optimal parts for your desired L@frequency or Z@frequency quickly, reducing your design cycle time.

Coilcraft's **MAGPro** suite of online inductor analysis tools are designed to enable inductor selection and circuit optimization based on sound engineering principles and measured data.

The RF Inductor/Choke Finder and Analyzer offers two search options. The L @ Frequency option identifies inductors suitable for your L, Q, and current requirements and displays

a full range of performance graphs including L, Q and ESR at frequency.

For RF choke applications, the Z@Frequency tool searches thousands of part numbers for your desired impedance and lets you select the desired choke based on size, performance, or a combination of the two.

Reduce your design cycle time with confidence at [www.coilcraft.com/tools](http://www.coilcraft.com/tools).

**Coilcraft®**

[WWW.COILCRAFT.COM](http://WWW.COILCRAFT.COM)

areas required at the core of the new E/E architecture.

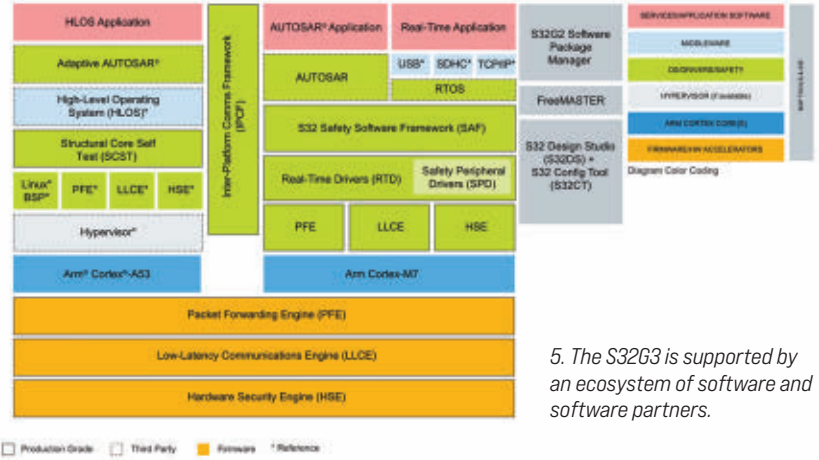
The first is functionally safe processing, covered by up to four lockstep Arm Cortex-M7 microcontrollers and up to eight cluster lockstep Arm Cortex-A53 microprocessors. These provide configurable ASIL D lockstep clusters and two ASIL B independent clusters.

On startup, memory and logic built-in self-test (BIST) check for possible issues, while a fault collection and control unit (FCCU) monitors operation, placing the device in a safe state should a failure be detected. Peripherals can also be assigned to specific cores at boot, enabling virtualization and containerization that supports fast startup and follows strict orchestration rules. This ensures, in hardware, that resources can't be impacted by code execution failures elsewhere on the device. Demonstration applications have already been created that use K3s for containerization.

High-speed communication is essential to SDVs, from daily operations to OTA updates. This brings us to the second core area: networking. However, the interrupts associated with CAN/CAN-FD, Ethernet, and others make determinism challenging.

To counteract this, the S32G3 offers a Low Latency Communication Engine (LLCE) complete with its own cores for handling legacy networks (CAN, FlexRay, LIN, and SPI). It includes offloading for AES encryption, time synchronization (IEEE 802.1AS), and flexible buffering. For Ethernet, up to three 2.5-Gb MACs are integrated into a separate Packet Forwarding Engine (PFE) supporting IEEE 1588v2 and AVB/TSN for deterministic communication. Further automotive interfaces and two PCI Express (PCIe) 3.0 interfaces (two lanes each) are available, too.

The third and final piece is security, starting with an advanced Hardware Security Engine (HSE). Integrating typical cryptographic functions (AES, SHA, ECC, RSA), it meets current security specifications such as E-safety Vehicle Intrusion Protected Application (EVITA).



5. The S32G3 is supported by an ecosystem of software and software partners.

*By establishing a root-of-trust at boot time, the processor ensures all modern security mechanisms are available that limit attacks and make certain only certified software and updates can be deployed to the vehicle.*

By establishing a root-of-trust at boot time, the processor ensures all modern security mechanisms are available that limit attacks and make certain only certified software and updates can be deployed to the vehicle. Finally, hardware support for Intrusion Detection and Prevention Systems (IDPS) with communication packet filtering and inspection help detect cyberattacks that can circumvent authentication and encryption mechanisms.

Development is accelerated with a range of hardware platforms (RDB3, GoldBox 3), enablement software from NXP and its partners (Fig. 5), along with the Vehicle Integration Platform (GoldVIP) supporting rapid connected gateway development and proof-of-concept efforts.

**Processors Ready for SDVs**

SDVs make huge promises to the public, both to those who want to own and those who only want to use personal transport. It's clear that the current approach of connecting 150 ECUs with different hardware and software from various suppliers can't deliver this vision.

OEMs are taking over the software development for their vehicles, leveraging new E/E architectures that can support the CI/CD workflows needed for the continuous rollout of new features and updates. Much of this process can be copied from existing cloud software development processes.

However, they must also be tuned to the vehicle's deterministic, functionally safe environment and the unique cybersecurity needs of automotive. New generations of ASIL D processors with hardware that simplifies virtualization and containerization, coupled with state-of-the-art security, are ready to take on this massive challenge. ■

**REFERENCES**

1. <https://k3s.io/>
2. <https://www.soafee.io/>
3. <https://www.tttech-auto.com/knowledge-platform/open-caros-and-software-defined-vehicle>

# Solutions That Are Above and Beyond



Rubidium™ MG362x1A

## The Source of Purity, Power, and Stability

Unmatched output power and best in class signal purity and frequency stability

Signal purity, output power, and frequency stability are essential distinguishing characteristics of a high-frequency microwave signal generator. The Rubidium MG362x1A signal generator is built to deliver these distinguishing characteristics across a broad frequency range and at high output power levels. With comprehensive AM, FM, PM, and pulse modulation capabilities, Rubidium offers performance unmatched in today's market.



Highest Output Power



VectorStar™ ME7838x

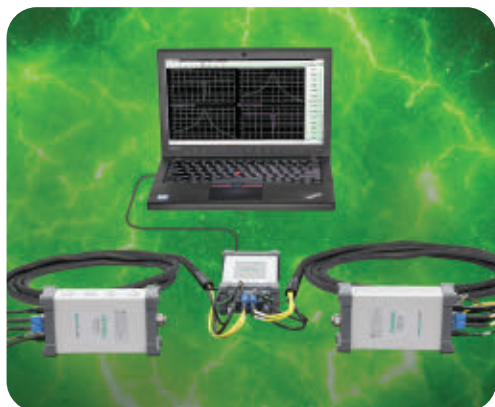
## Excellence in mmWave Measurements

The world's first 4-port 70 kHz to 220 GHz single-sweep VNA/SPA with differential probes

Building on more than 40 years of design experience, Anritsu has broken the millimeter-wave barrier with the VectorStar ME7838x series VNA/SPA. RF and microwave engineers now have access to a powerful measurement tool for performance analysis of devices ranging from transistors in an on-wafer environment to communication systems, as well as opto-electronics to 100 GHz.



Broadest Frequency Coverage to 220 GHz



ShockLine™ ME7869A

## Full Vector S-parameter Measurements

Conduct full vector S-parameter measurements at wide distances of 100 meters or more

Powered by PhaseLync™ technology, the ShockLine™ ME7869A enables engineers to synchronize two portable ShockLine MS46131A modular VNAs and connect them to a DUT or AUT to conduct vector transmission measurements over distances of up to 100 meters, and at a lower cost. PhaseLync™ synchronization eliminates the need for long testport cable runs while simplifying set up and improving dynamic range and stability of S-parameter measurements in OTA and other long distance applications.



PhaseLync Technology

**Anritsu**  
Advancing beyond

Discover how you can achieve measurement excellence with Anritsu. Visit [www.anritsu.com/test-measurement](http://www.anritsu.com/test-measurement)



# An Introduction to the VNA and Vector Network Analysis

This article provides a brief tutorial on the vector network analyzer, how it works, and its application.

By *Brian Walker*, Senior RF Engineer SME, Copper Mountain Technologies

Most design engineers are familiar with tools of the trade such as voltmeters, oscilloscopes, signal generators, and spectrum analyzers. Some may not have had the opportunity to use a vector network analyzer (VNA). It's the intent of this article to introduce VNA measurement and present a few typical applications.

## Why is a VNA Useful?

Transmission lines can support RF propagation in either direction. Signals traveling along a transmission line may encounter localized impairments that aren't precisely 50 Ω, such as connectors or transitions from coaxial to planar media (other impedances such as 75 Ω are common, but for the purposes of this explanation we will use 50 Ω). Each impairment gener-

ates a reflection that travels back toward the source along the transmission line.

A 50-Ω load on the end of a 50-Ω transmission line absorbs all signal energy and reflects nothing. Any load other than 50 Ω will generate some amount of reflection. The farther the load is from 50 Ω, the greater the reflection. A short and an open circuit reflect the entire signal back to the source. To characterize reflections, we introduce the *reflection coefficient* ( $\Gamma$ ):

$$\Gamma = \frac{z - z_0}{z + z_0}$$

where  $z_0$  is the characteristic impedance of the source and transmission line and  $z$  is the complex impedance of the load.

If  $z$  is 0—a short—then  $\Gamma = -1$ , or a complete reflection that's 180 degrees out of phase with the incident signal. If  $z$  is infinite—an open—then  $\Gamma = 1$ , or a complete reflection in phase with the incident signal. If  $z = z_0$ —a 50- $\Omega$  load—then  $\Gamma = 0$ , which means no reflection at all.

A VNA can separate and measure incident and reflected signals, and thus directly determine reflection coefficients. *Figure 1* depicts a VNA measurement. The incident signal exits the VNA from Port 1 and arrives at the input to the device under test (DUT). At that interface, there may be some reflection that returns to Port 1. The remainder of the signal passes through the DUT and enters Port 2 of the VNA. Two receivers at Port 1 measure both incident and reflected waves, and a receiver at Port 2 measures the wave entering there.

We call the ratio of the incident wave to the reflected wave—the reflection coefficient— $S_{11}$ . The ratio of the signal entering Port 2 to the incident signal leaving Port 1 is called  $S_{21}$ . *Figure 1* shows both.

In the real world, there would be reflections from within the DUT and another reflection at the output connector, but they're not shown to keep the diagram simple.

There are only a few possibilities for what can happen to the incident signal:

- It can be reflected back to the source in one or more places.
- It can be dissipated as heat within the DUT.
- It can be radiated away by the DUT.
- It can pass through the DUT and make its way to Port 2.

If the signal isn't dissipated or radiated, then a direct relationship exists between  $S_{21}$  and  $S_{11}$ . That is:

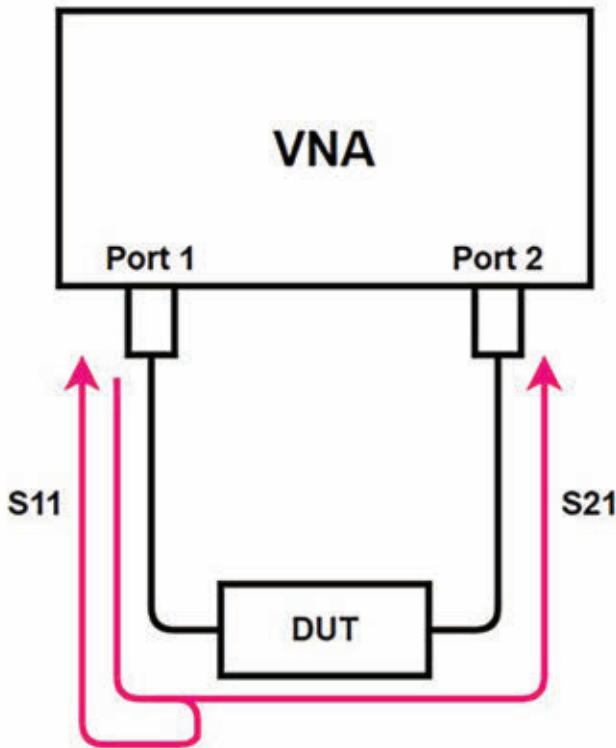
$$S_{21}^2 = 1 - S_{11}^2$$

This is simply a conservation of energy statement. Signals that aren't being reflected must pass through the DUT.

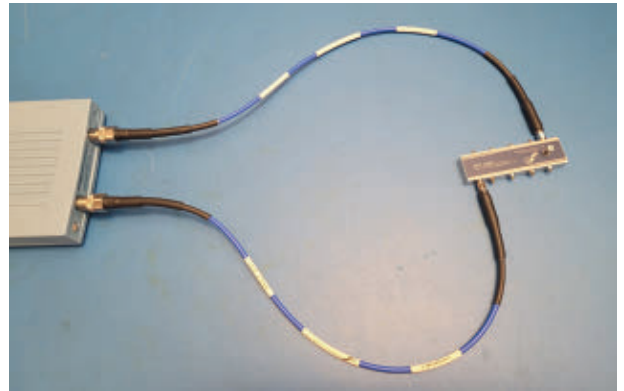
### What Does a VNA Measurement Look Like?

In the actual measurement, a 4-GHz bandpass filter is connected to an SC5090, a 9-GHz 2-port analyzer (*Fig. 2*).

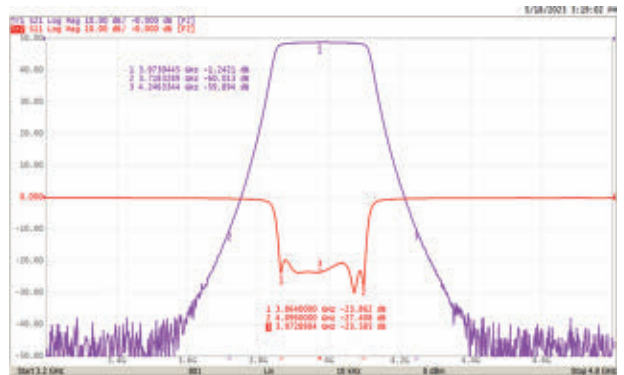
The purple trace in *Figure 3* shows  $S_{21}$  in log magnitude format. This is the signal that passes through the filter from Port 1 to Port 2. Markers 2 and 3 indicate the points at which the



1. A VNA can separate and measure incident and reflected signals; therefore, it's able to directly determine reflection coefficients. Shown here is a simplified VNA measurement setup. Images courtesy Copper Mountain Technologies



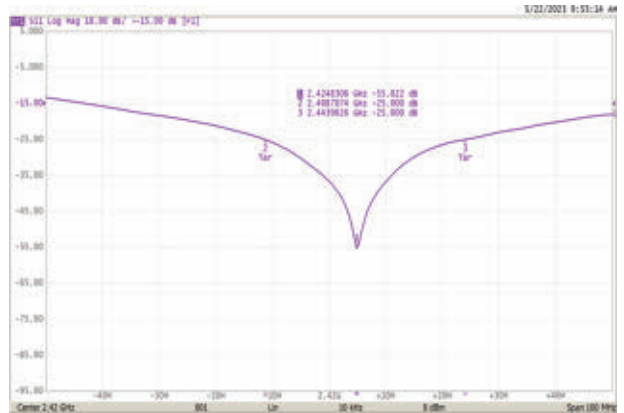
2. In the actual measurement depicted in *Figure 1*, a 4-GHz bandpass filter is connected to an SC5090, a 9-GHz two-port analyzer.



3. Shown are the measurement results for the 4-GHz bandpass filter.



4. This is the measurement setup for a Wi-Fi antenna that receives and transmits in the 2.4-GHz band.



5. A one-port measurement of the antenna in Figure 4 shows a sharp dip in  $S_{11}$  at 2.42 GHz and reasonably low values across the measurement range.

filter attenuation is 60 dB. Marker 1 is set to the middle of the filter, where most of the signal is passing with little attenuation.

In this chart, the dB scale on the left side is relevant to the red  $S_{11}$  trace, and the zero for  $S_{21}$  is at the top of the screen. The markers show actual values.

The red trace shows  $S_{11}$ , which is the reflection from the filter. In places where the filter isn't passing the signal, it's being completely reflected. In this case, 0 dB is equal to a linear "1," or complete reflection. In the places that have almost no reflection—where  $S_{11}$  is less than -20 dB—the signal is passing through the filter with very little loss.

When speaking of filters, the measurement through the filter—the *insertion loss*—is the  $S_{21}$  reading within the passband and the *return loss* is the  $S_{11}$  measurement in the passband. Here, the insertion loss is 1.2 dB in the middle of the passband, and the return loss is better than 20 dB. Both numbers are traditionally stated as positive values, even though the S-parameters themselves are negative.

Figure 4 shows measurements being taken on a Wi-Fi antenna. This antenna receives and transmits in the 2.4-GHz band. A one-port measurement of the antenna reveals a sharp dip in  $S_{11}$  at 2.42 GHz and reasonably low values across the measurement range (Fig. 5).

Because  $S_{11}$  shows very little reflection—or high return loss—across the Wi-Fi band, the stimulus signal from the VNA must be efficiently radiating away. This antenna is therefore functioning properly.

### The Touchstone Matrix

$S_{11}$  represents the ratio of the reflection back to Port 1 to the signal emitted by Port 1, and  $S_{21}$  is the ratio of the signal measured at Port 2 to the signal emitted by Port 1. Similarly,  $S_{22}$  is the ratio of the signal reflected back to Port 2 to the signal emitted by Port 2, and  $S_{12}$  is the ratio of the signal measured at

Port 1 to the signal emitted by Port 2. These last two might be called *reverse* measurements, as the signal is being emitted by Port 2 instead of Port 1.

If all four S-parameters are known over frequency for a linear two-port DUT, then this represents a complete characterization of the device. The S-parameters, saved in Touchstone format, may be used in a linear simulator to study how the DUT will behave with various RF excitations and loads.

### Conclusion

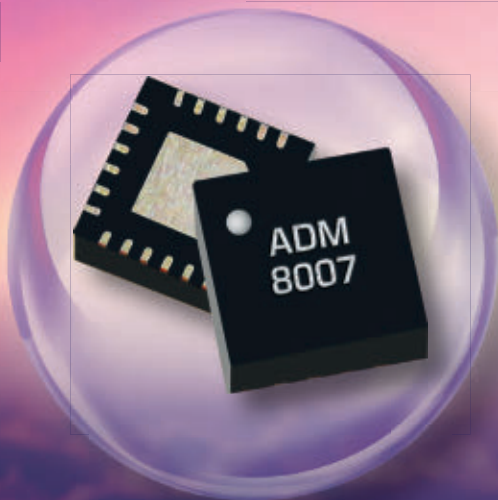
The VNA measures the RF properties of a DUT by emitting an RF voltage wave and subsequently measures how much of it is reflected and how much passes through the DUT for a two-port measurement. For a one-port measurement, it simply measures the reflected wave. A low reflection means that the signal enters the DUT and very little returns.

Measurements such as that may be performed to determine the function and suitability of an unknown device or to create a Touchstone file for use in linear simulation. This makes the VNA a very powerful tool for the RF engineer.

Copper Mountain Technologies produces a wide range of VNAs with output frequencies from 1.3 to 330 GHz. Visit [www.coppermountaintech.com](http://www.coppermountaintech.com) for product information and educational articles and videos on vector network analysis. ■

# PERFORMANCE THAT SEEMS UNREAL

ADM-8007PSM  
2-40 GHz  
Surface Mount  
Amplifier



Marki Microwave continues to lead in performance with the ADM-8007PSM. The cost-competitive solution combines two amplifier stages into a single package, making it capable of providing sufficient LO drive to power a wide variety of mixers to 40 GHz when driven with an input power of 0 to +5 dBm. Ideal for mobile test and measurement equipment, radar, satcom, and 5G transceivers, it is available as a 4x4 mm QFN.

- **+23 dBm output power**
- **23 dB flat gain response**
- **4 dB noise figure**
- **Single 5V supply, no external bias tee required**

Contact: [sales@markimicrowave.com](mailto:sales@markimicrowave.com)  
[www.markimicrowave.com](http://www.markimicrowave.com)

*The Trusted Leader When Performance Matters*



# State-of-the-Art Testers Chase Complex Wireless Signals

As wireless applications and frequencies ramp up, test equipment must increase measurement capabilities, even when operating as battery-powered portables, into the mmWave range.

By **Jack Browne**, Technical Editor

**WIRELESS TECHNOLOGY IS** synonymous with RF and microwave signal frequencies, although it's steadily moving higher in frequency into the millimeter-wave (mmWave) range. As a result, the test equipment needed to design, develop, and maintain wireless products must constantly evolve to higher frequencies and more advanced signal formats.

With ever-increasing numbers of wireless products in use, competition grows for available frequency spectrum. It's essential for testing to ensure that wireless devices designed to emit signals don't exceed their limits and interfere with nearby equipment. Fortunately, high-frequency test-equipment suppliers represent an innovative group that has developed effective measurement solutions for wireless testing. A sampling of such test gear is reviewed here.

Wireless equipment and systems are rapidly filling frequency spectrum, into the mmWave range and beyond. Growing demand for wireless electronic products is driving the development of test equipment capable of generating and analyzing complex signals quickly, over broad bandwidths for versatility.

As wireless products grow smaller in size with increasing functionality, networks must handle more of these devices simultaneously and wrestle with issues such as signal distortion and interference. Consequently, test-equipment developers are prompted to create instruments that can closely imitate the performance of any device under test (DUT) that they evaluate, even wireless gear that may be operating from a satellite.

The collection of wireless testers that follows provides a small sample of measurement equipment designed to maintain the operation of wireless applications as they embrace users worldwide.

## 5G Test Equipment

Fifth-generation (5G) New Radio (NR) wireless cellular networks are among the most visible of wireless applications. They connect portable telephones by the billions and add Internet of Things (IoT) sensors and other devices in commercial, industrial, medical, and military markets in large numbers.

Many wirelessly connected devices require greater numbers of base stations and wireless-local-area-network (WLAN) access points as well as additional frequency bandwidth. As 5G networks extend from the sub-6-GHz frequencies of frequency range 1 (FR1) to the mmWave frequencies of frequency range 2 (FR2), test-equipment developers race to provide the signal analyzers and generators that can cover the frequency ranges for 5G's many channels, from 410 to 7125 MHz for FR1 and 24.25 to 71.00 GHz for FR2.

Over-the-air (OTA) testing of 5G networks requires signal-analysis capability across increasingly broadband frequency ranges extending to mmWave frequencies. As an example, the [Field Master Pro](#)



1. Portable RTSAs such as the *Field Master Pro MS2090A* provide the frequency range and measurement capability to support wireless in-field testing through mmWave frequencies. Anritsu

**MS2090A** real-time spectrum analyzer (RTSA) from [Anritsu Co.](#) is available in versions covering ranges between 9 kHz to 9 GHz and 9 kHz to 54 GHz, with natural mechanical differences such as Type N connectors in the 9-GHz version and 1.85-mm V connectors in the 54-GHz version. All offer a 5G NR demodulation mode to ease 5G wireless testing.

These compact portable analyzers (*Fig. 1*) function for about two hours on a battery charge and show results on a 10.1-in. color touchscreen display screen. With analysis bandwidths as wide as 110 MHz, they're as well-suited for wireless communications measurements such as for pulsed radar testing. The RTSAs can perform a variety of test applications, including broadband transmitter signal analysis, satellite-communications (satcom) system monitoring, microwave radio-link testing, and spectrum monitoring and interference hunting.

When equipped with a preamplifier, the analyzers can detect and display extremely low-level signals, for example from a test antenna, by merit of a displayed average



noise level (DANL) of  $-164$  dBm. A free downloadable software tool for a PC simplifies remote spectrum monitoring.

Anritsu recently announced a solution to conformance testing of the multitude of devices that will occupy the 5G FR1 under-6-GHz frequency range—the [MR7873NR Lite](#) tester. It performs the 5G FR1 certification testing per Third-Generation Partnership Program (3GPP) communications standards.

It accounts for the scheduling of frequency bands for the many wireless functions supported by the multiple frequency bands within the sub-6-GHz FR1 range. The complete test system is capable of transmitting and receive testing for the many modulation formats of signals in wireless systems, including for cellular, WLAN, and IoT devices.

### More Analyzers Become Portable

[Keysight Technologies](#) offers a wide range of benchtop and portable/handheld spectrum and signal analyzers (as well as compact portable packages that combine analyzers with signal generators for comprehensive wireless testing). The [FieldFox handheld analyzers](#) weigh just 7.35 lbs. but are more like complete measurement laboratories than handheld spectrum analyzers.

Each battery-powered unit contains a swept-frequency spectrum analyzer, an RTSA, a GPS receiver, power meter, interference analyzer, and even offers an option for a vector network analyzer (VNA) to perform S-parameter measurements. Models come with frequency ranges as low as 30 kHz to 4 GHz and as high as 30 kHz to 54 GHz. The RTSAs can study analysis bandwidths as wide as 40 or 120 MHz and detect signals as brief as 47 ns.

With such broad frequency coverage, FieldFox portable analyzers are available for in-field OTA measurements within both frequency ranges (FR1 and FR2) of 5G wireless networks (*Fig. 2*). They feature excellent amplitude accuracy of  $\pm 0.2$  dB over broad dynamic ranges.

Using USB connections to a PC running the Keysight Spectrum Manage-



2. The FieldFox line of portable spectrum analyzers includes multifunction measurement tools with upper-frequency limits as high as 54 GHz in support of 5G wireless-network OTA testing. Keysight Technologies



3. This portable spectrum analyzer is available in versions with frequency coverage as wide as 5 kHz to 44 GHz and extremely wide dynamic ranges. Rohde & Schwarz



4. Portable RTSAs in the RSA7100A/B line offer acquisition bandwidths as wide as 800 MHz from 16 kHz to 26.5 GHz. Tektronix

ment Software (KSMS), the analyzers can implement a spectrum emission mask (SEM) to measure in-band and out-of-band EM energy within set bandwidths when searching for interference. The software supports various applications, including satcom monitoring. For chasing pulses, the analyzers can operate with video triggers and external triggers and set time gates from 6  $\mu$ s to 1.8 s.

The [R&S Spectrum Rider FPH](#) handheld spectrum analyzers (*Fig. 3*) from [Rohde & Schwarz](#) come in versions covering 5 kHz to 2 GHz and as high as 5 kHz to 44 GHz, all with 1-Hz frequency resolution. The instruments measure fre-

quency spans from 10 Hz to 600 MHz with sweep times ranging from 20 ms to 1000 s. RBWs can be set from 1 Hz to 3 MHz, and a DANL of  $-150$  dBm or better (with internal preamplifier) enables detection of low-level signals. The portable analyzers run as long as 4.5 h on a battery charge.

The company also developed its [R&S ESMW](#) ultrawideband monitoring receiver for spectrum monitoring from 8 kHz to 40 GHz. With real-time bandwidths as wide as 2 GHz, it's designed to capture broadband wireless signals even in highly populated, high-density spectrum environments.

The [RSA7100A](#) and [RSA7100B](#) RTSAs (Fig. 4) from [Tektronix](#) are available from 16 kHz to 14.0 GHz or 16 kHz to 26.5 GHz with standard maximum acquisition bandwidth of 320 MHz and optional maximum acquisition bandwidth of 800 MHz. The RTSAs measure signal levels as high as +30 dBm and as low as -145 dBm. Built-in attenuators provide as much as 75-dB attenuation to 26.5 GHz. The spectrum analyzers come with or without a GPS receiver and can perform a wide range of automatic measurements with the company's [SignalVu-PC software](#).

### Portable and Modular Testers

As electronic products are being designed for miniaturization with increased functionality, wireless test instruments are following that trend in portable and modular packages with increased measurement performance and capabilities for their small sizes.

For example, the [model SP145](#) from [Signal Hound](#) packs multiple measurement functions, including a swept-frequency spectrum analyzer and RTSA, into a compact portable unit operated by software on a PC via USB connections (Fig. 5). It has a frequency range of 100 kHz to 14.5 GHz and sweep speeds to 200 GHz/s to capture even brief signal events over wide frequency spans. With a DANL of -160 dBm, it can detect and display low-level signals of interest.

Supplied with the company's free Spike test software, it's compatible with PCs containing MS Windows or the Linux operat-



5. This single enclosure houses several spectrum analyzers and wireless testers for applications from 0.1 MHz to 14.5 GHz. [Signal Hound](#)

ing system (OS). [Signal Hound](#) recently announced its [model SM435B/C RTSAs](#) with frequency coverage into the mmWave range, from 100 kHz to 43.5 GHz.

[Siglent](#) is another supplier of portable handheld spectrum analyzers suitable for wireless testing. The [SSA5000A](#) series analyzers cover a range of 9 kHz to 26.5 GHz. They can work as spectrum analyzers to gauge signal amplitudes and as vector signal analyzers and transceivers to study signal amplitude and phase.

Modular systems such as the [PXIe-5644 vector signal transceiver \(VST\)](#) from [NI](#) test wireless systems with massive-input, massive-output (MIMO) antenna configurations. The VST's PXI format enables users to slide modules as needed into a mainframe chassis to achieve the required measurement capability.

### Dealing with Signal Overlap

As the density of wireless devices and their signals increases, opportunities for signal overlap and interference also expand, such as between 5G and WLAN systems with Wi-Fi equipment based on the IEEE 802.11 protocol. With WLANs operating in the unlicensed ISM band along with similar short-range wireless technologies such as Bluetooth and Zigbee, WLAN testing helps ensure stable operation in such dense signal environments.

The latest (sixth) generation of Wi-Fi devices (Wi-Fi 6E) reach 7.125 GHz. Wireless testers for evaluating WLAN signals and products must support applications extending higher in frequency (the seventh Wi-Fi generation is under development) and sharing spectrum with other wireless devices. A microwave oven leaking EM energy at 2,450 MHz, for example, can degrade the performance of a WLAN receiver.

Many of the spectrum analyzers reviewed earlier can act as Wi-Fi or WLAN receivers to analyze signal quality in a WLAN system. When more specialized test solutions are required, equipment such as the [model MT8862C Wireless Connectivity Test Set](#) from [Anritsu Co.](#) is well-suited to evaluate the perfor-

*Many of the spectrum analyzers reviewed earlier can act as Wi-Fi or WLAN receivers to analyze signal quality in a WLAN system.*

mance of DUTs under typical WLAN operating conditions.

The [MT8862C](#) is a benchtop instrument with multiple test channels and frequency bands required for IEEE 802.11 WLAN testing, supporting testing at 2.4- and 5.0-GHz WLAN frequency ranges. It can be set for the many channels defined by the protocol within both frequency ranges and characterizes data rates to 54 MB/s possible with WLAN's orthogonal-frequency-division-multiplex (OFDM) transmissions. It's able to test WLAN DUTs and access points; two of the test sets can be combined for 2 × 2 MIMO testing.

The [CMP180 Radio Communications Tester](#) from [Rohde & Schwarz](#) performs Wi-Fi 6E and 5G cellular testing to 8 GHz, including MIMO antenna testing. It incorporates two separate vector signal generators and two vector signal analyzers as well as a power supply and controller within a compact housing. Each of the two RF channels has eight ports for a total of 16 RF test ports with bandwidths as wide as 500 MHz.

Another test platform for Wi-Fi 6E is the [E6680E Wireless Test Set](#) from [Keysight Technologies](#). It also has 16 RF ports for testing multiple antennas and MIMO configurations. It combines a vector signal analyzer and vector signal generator both with a CW frequency range of 380 to 7,535 MHz and 1-Hz frequency resolution. The compact test set delivers a wide dynamic range for its broad frequency coverage, from -70 to +30 dBm, with ±0.75 dB or better amplitude accuracy.

The company has also developed portable testers that operate according to the IEEE 802.11 WLAN communications protocol. One example is the [AV1021A](#)

# WEST·BOND's New 7KF

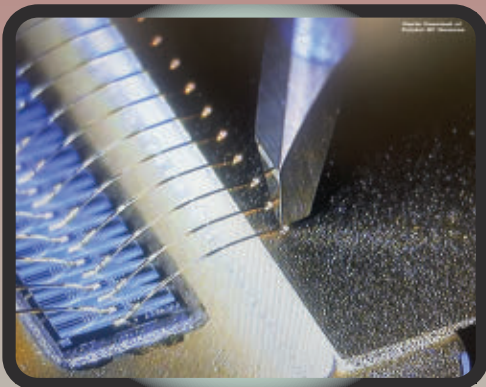


[www.westbond.com](http://www.westbond.com)

*Helping you make that crucial connection since 1966*

7KF Wedge-Wedge and Ball Wedge wire bonding system:

- 7" Capacitive Touch Screen
- Programmable Force and Tool Heat
- Primary and Secondary Ball Size Control
- Cu Ball Option Available
- Cortex M7 Microcontroller
- High and Low Frequency



## WEST·BOND®

1551 S. Harris Court Anaheim, CA 92806  
Ph. (714) 978-1551  
E-Mail: [sales@westbond.com](mailto:sales@westbond.com)





6. This compact signal generator runs on AC or battery power and provides test signals to 26.5 GHz with 0.001-Hz frequency resolution. Berkeley Nucleonics

**WaveBee Touch handheld analyzer** for vehicle-to-vehicle (V2V) and vehicle-to-everything (V2X) mobile wireless communications testing.

### Generating Signals

Many companies developing wireless signal analyzers produce signal generators that enable emulation of modulated signals within wireless systems. For example, **Berkeley Nucleonics Corp.** may not be known for a WLAN analyzer, but the firm does produce the **845 fast-switching microwave signal generator** (Fig. 6) with all major modulation formats. In addition, modulation such as amplitude modulation (AM) and pulse modulation can be combined to create signals for realistic radar devices and system testing.

The signal generator comes in versions from 9 or 100 kHz to 12.0, 20.0, or 26.5 GHz with impressive 0.001-Hz frequency resolution. Signal power ranges from -20 to +15 dBm in standard models, with an option for -90 to +25 dBm. Both ranges can be adjusted with 0.01-dB resolution. The signal source has 400- $\mu$ s standard switching speed, which can be accelerated to 30  $\mu$ s as an option. While the flexible signal generator runs on standard AC power, it can also operate on battery power for in-field measurements.

The **SMB100A signal generator** from Rohde & Schwarz is also available in multiple versions from 100 kHz to 12.75,



7. The standard high-frequency ceiling of 40 GHz for the SMB100A signal generator can be raised to 110 GHz with a frequency multiplier. Rohde & Schwarz

20.00, 31.80, or 40.00 GHz, and can be extended to 110 GHz with a frequency multiplier (Fig. 7). It's well-equipped with modulation, including pulse modulation, and can control signal output-power levels from -120 to +27 dBm (for units with a step attenuator). The **VXG M9384B** and **VXG-m M9383B signal generators** from Keysight Technologies come in versions covering 1 MHz to 14.0, 20.0, 31.8, or 44.0 GHz with 0.01-Hz frequency resolution and 0.01-deg. phase control of a  $\pm 180$ -deg. phase range.

### Testing Services

In crowded operating environment, such as large cities, wireless applications like 5G and Wi-Fi may overlap in frequency and wireless products must be tested according to standards including ANSI C63.27 to ensure their wireless coexistence capabilities. Fortunately, rather than selling test equipment, some companies offer wireless testing services for applications such as 5G and Wi-Fi, or wireless coexistence testing.

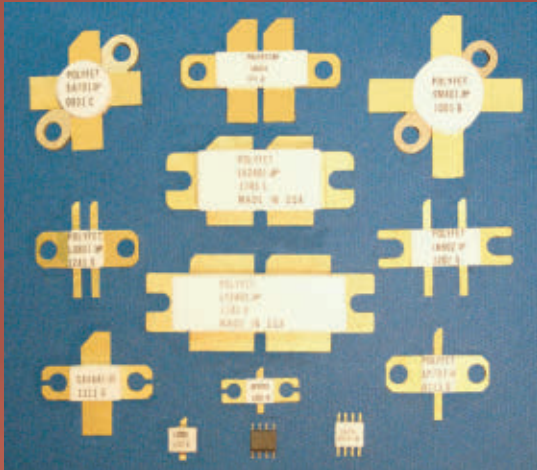
**Spirent** is known for extensive Wi-Fi test services, while **F2 Labs** performs UL and CSA certifications as well as FCC Part 15 certifications for wireless emitters including Wi-Fi. Eurofins MetLabs provides test services for U.S. and international wireless system requirements. And **RF Exposure Lab** has been certified for test services through mmWave frequencies.

**GL Communications Inc.** offers services and equipment for voice, data, and video testing of mobile wireless networks including 5G systems. Performance and conformity testing can be combined during 5G drive testing in a car. The firm's **Universal Test Platform** holds as many as six modules for different combinations of wireless test functions, while its **Message Automation and Protocol Simulation (MAPS) software** supports a variety of wireless-communications protocols, including satcom echo delay measurements.

For wireless measurement applications that can be performed periodically, test equipment rentals provide a way to acquire the measurement capability needed for an application while avoiding obsolescence as wireless frequency bands continue to increase. Companies offering test-equipment rentals include **Axiom Test Equipment**, **ElectroRent**, and **TRS-Rentelco**.

Wireless testing sometimes requires connecting cables, such as with the **TXG200 WLAN network test kit** from Platinum Tools. The kit tests copper and fiber-optic cables in WLAN systems. It can measure Wi-Fi signal strength and cable lengths within a network and perform Ethernet speed certifications to 10 Gb/s. The kit includes the company's XG2 tester, chargers, patch cables, and carrying case. ■

# Broadband RF power transistors, modules, and evaluation amplifiers: Polyfet RF Devices offers them all.

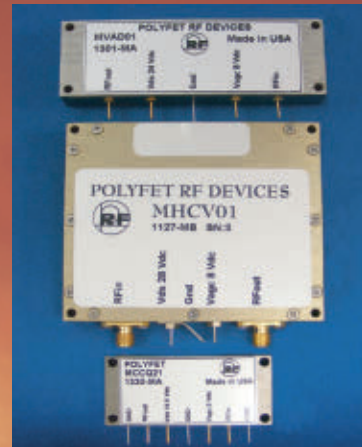


**GaN:** 28VDC and 48VDC, up to 3GHz, up to 160W, single-ended and push-pull.

**LDMOS:** 5-50VDC, up to 1.5GHz, up to 2kW, single-ended and push-pull.

**VDMOS:** 12.5-50VDC, up to 1GHz, up to 400W, single-ended and push-pull.

**Broadband RF power modules:**  
Utilize GaN and D-MOS technologies.  
24-48VDC, up to 1260MHz, up to 350W CW,  
various case sizes and RF connection types.  
Custom design requests welcomed.



**Various evaluation amplifiers available:**  
Displayed here is the TB280. It demonstrates the LY2542V (LDMOS) putting out 1kW, 22dB across 88-108MHz with 50VDC supply.



Your  
Power  
MOSFET  
People

**polyfet rf devices**

[www.polyfet.com](http://www.polyfet.com)

TEL (805)484-4210

# Phase-Noise Modeling, Simulation, and Propagation in Phase-Locked Loops (Part 2)

In Part 2, we design a hypothetical PLL frequency synthesizer as an example to be used for analysis.

By **Frederick Weist**,  
Principal, FCW Sciences



Lightpoet\_110416218 | Dreamstime

**A**s noted in [Part 1](#), phase-locked loops (PLLs) are ubiquitous in today's high-tech world. Almost all commercial and military products employ them in their operation and phase (or PM) noise is a major concern. Frequency (or FM) noise is closely related (instantaneous frequency is the time derivative of phase) and is generally considered under the umbrella of phase noise (perhaps both might be considered "angle noise"). Amplitude (or AM) noise is another consideration.

While both affect PLL performance, amplitude noise is usually self-limiting and of no consequence. Phase noise, therefore, at the PLL output and of the RF components, is the dominant concern. Of course, output phase noise is the ultimate concern and depends critically on the phase noise of each component. A number of factors contribute to component phase noise, such as power supplies, EMI, and semiconductor anomalies, to name a few, and understanding these factors allows us to implement mitigation strategies for component phase noise and, ultimately, output phase noise.

Part 1 discussed brief theory and typical measurements of phase noise along with the analysis (modeling, simulation, and propagation) thereof, and showed the method used by most computer-aided-design (CAD) applications. Part 2 digs into the design of a hypothetical PLL frequency synthesizer to be used for analysis.

## Design of 8- to 12-GHz Output/50-MHz Step PLL Frequency Synthesizer

To demonstrate the concepts and methods reviewed in Part 1, we design a hypothetical single loop 8- to 12-GHz/50-MHz step (channel spacing) integer synthesizer with a 25-MHz reference

(50 MHz being the smallest achievable step since, looking ahead, we will use a fixed modulus divide-by-2 prescaler). It will be designed for the lowest average output phase noise across the band by achieving the lowest phase noise at the 10-GHz mid-band output. We follow a standard design procedure:

### 1. Review specifications.

For this example, the sole specification is phase noise (an impractical oversimplification explicitly for this example) as described above.

### 2. Select circuit configuration, type, order, and loop-filter topology.

Discrete (rather than IC or hybrid) configuration, Type 2, second-order with first-order active PI loop filter (chosen because of its simplicity and popularity).

### 3. Select components.

*Reference:* Prominent electronics manufacturer's 100-MHz OCVCXO (Figs. 5 and 6).

*Reference Divider:* Prominent electronics manufacturer's Programmable Integer Divider with range  $K_I (= 1/R) = 1/1$  to  $1/17$  ( $R = 1$  to  $17$ ) programmed to:

$R = 4$  at All GHz

*Feedback Divider:* Prominent electronics manufacturer's programmable integer/fractional divider used in integer mode with range  $K_m (= 1/M) = 1/32$  to  $1/1048575$  ( $M = 32$  to  $1048575$ ) programmed to:

- M = 160 at 8 GHz
- M = 180 at 9 GHz
- M = 200 at 10 GHz
- M = 220 at 11 GHz
- M = 240 at 12 GHz

**Prescaler:** Prominent electronics manufacturer's fixed modulus divide-by-2 prescaler with  $K_p (= 1/P) = 1/2$  ( $P = 2$ ) giving total feedback factor of  $K_n (=1/N) = 1/MP$  ( $N=MP$ ) producing:

- P = 2 at All GHz
- N = MP = 320 at 8 GHz
- N = MP = 360 at 9 GHz
- N = MP = 400 at 10 GHz
- N = MP = 440 at 11 GHz
- N = MP = 480 at 12 GHz

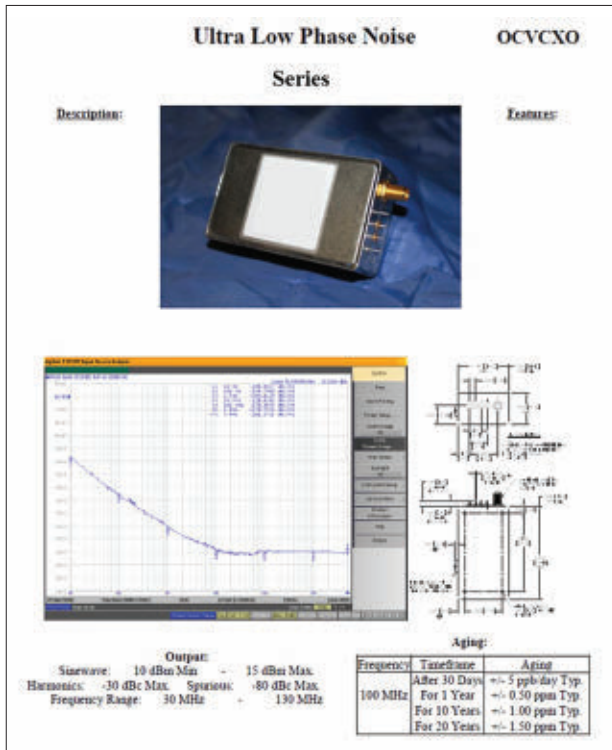
**VCO:** Prominent electronics manufacturer's 8- to 12.5-GHz low-noise VCO<sup>11</sup> with:

- $K_v = 900 \text{ MHz/V}$  [ $5.7(10^9) \text{ rad/S/V}$ ] at 8 GHz
- $K_v = 825 \text{ MHz/V}$  [ $5.2(10^9) \text{ rad/S/V}$ ] at 9 GHz
- $K_v = 725 \text{ MHz/V}$  [ $4.6(10^9) \text{ rad/S/V}$ ] at 10 GHz
- $K_v = 540 \text{ MHz/V}$  [ $3.4(10^9) \text{ rad/S/V}$ ] at 11 GHz
- $K_v = 375 \text{ MHz/V}$  [ $2.4(10^9) \text{ rad/S/V}$ ] at 12 GHz

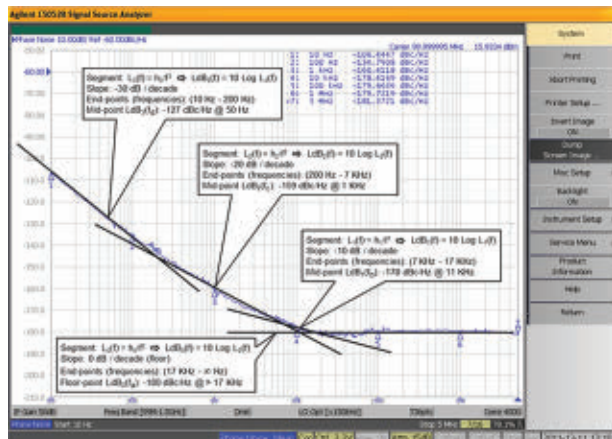
**Phase Detector:** Prominent electronics manufacturer's phase/frequency detector (PFD) with gain-control circuit to compensate for  $K_v$  variations across the VCO band (maintaining  $K_\phi K_v = \text{constant}$ ) to produce effective:

- $K_\phi = 0.134 \text{ V/rad}$  at 8 GHz
- $K_\phi = 0.147 \text{ V/rad}$  at 9 GHz
- $K_\phi = 0.166 \text{ V/rad}$  at 10 GHz
- $K_\phi = 0.225 \text{ V/rad}$  at 11 GHz
- $K_\phi = 0.318 \text{ V/rad}$  at 12 GHz

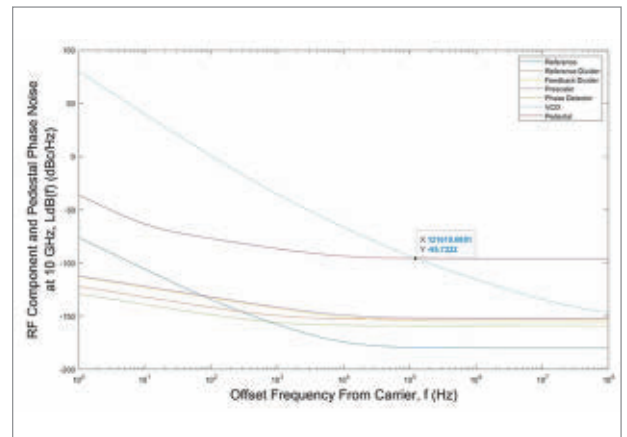
**Loop filter/Error amplifier:** Prominent electronics manufacturer's op amp (with adequate gain, precision, noise, bandwidth, stability, power-supply requirements, and output-voltage/current-drive capabilities).



5. Reference [100-MHz OCVCXO] datasheet from manufacturer for 8- to 12-GHz output/50-MHz step PLL frequency synthesizer. Images courtesy FCW Sciences



6. Reference [100-MHz OCVCXO] phase-noise plot (Fig. 5) with General Phase Noise Model (Fig. 3 from Part 1) fit to plot for 8- to 12-GHz output/50-MHz step PLL frequency synthesizer.



7. RF component and pedestal phase noise at 10-GHz mid-band output showing optimal loop bandwidth,  $f_g$ , at VCO/pedestal intersection for 8- to 12-GHz output/50-MHz step PLL frequency synthesizer.

#### 4. Develop phase-noise models for the RF components.

We use steps 1 to 6 of our *Phase Noise Analysis Procedure* (from Part 1) to develop the RF component phase-noise models and simulate them in *Figure 7*. We show the complete development for the Reference including the *General Phase Noise Model* (*Fig. 3, Part 1*) fitted to its datasheet phase-noise plot (*Figs. 5 and 6*) along with its calculations and resulting specific phase-noise model.

For the other components, we only show their calculations and resulting specific phase-noise models for brevity (also, for simplicity, the loop filter/error amplifier isn't modeled since it's not an RF component and its analysis is more complex than that for an RF component<sup>1</sup>):

##### A. Reference (at 100 MHz)

Phase-noise model points,  $LdB_j(f_i)$ , from fitting *General Phase Noise Model* to datasheet plot:

- Floor Segment: 0 dB/dec (17 kHz - ∞ Hz)
- Floor-point:  $LdB_0(f_a) = -180$  (17 kHz) (dBc/Hz)
- $L_0(f_a) = 10^{LdB_0/10} = 10^{-18.0}$  (17 kHz) (volts\_ratio<sup>2</sup>/Hz)
- Flicker Segment: -10 dB/dec (7 kHz - 17 kHz)
- Mid-point:  $LdB_1(f_b) = -178$  (11 kHz) (dBc/Hz)
- $L_1(f_b) = 10^{LdB_1/10} = 10^{-17.8}$  (11 kHz) (volts\_ratio<sup>2</sup>/Hz)
- Flicker Segment: -20 dB/dec (200 Hz - 7 kHz)
- Mid-point:  $LdB_2(f_c) = -159$  (1 kHz) (dBc/Hz)
- $L_2(f_c) = 10^{LdB_2/10} = 10^{-15.9}$  (1 kHz) (volts\_ratio<sup>2</sup>/Hz)
- Flicker Segment: -30 dB/dec (10 Hz - 200 Hz)
- Mid-point:  $LdB_3(f_d) = -127$  (50 Hz) (dBc/Hz)
- $L_3(f_d) = 10^{LdB_3/10} = 10^{-12.7}$  (50 Hz) (volts\_ratio<sup>2</sup>/Hz)

Phase-noise model coefficients,  $h_j$ , from above phase-noise model points:

- $h_0 = L_0 f_a^0 = 10^{-18.0}$  (volts\_ratio<sup>2</sup>Hz<sup>-1</sup>)
  - $h_1 = L_1 f_b^1 = (10^{-17.8})(11(10^3))^1 = 10^{-13.8}$  (volts\_ratio<sup>2</sup>)
  - $h_2 = L_2 f_c^2 = (10^{-15.9})(10^3)^2 = 10^{-9.9}$  (volts\_ratio<sup>2</sup>Hz)
  - $h_3 = L_3 f_d^3 = (10^{-12.7})(5(10^1))^3 = 10^{-7.6}$  (volts\_ratio<sup>2</sup>Hz<sup>2</sup>)
- Phase-noise model,  $LdB_{xi}(f)$ , from above coefficients:

$$L_{xi}(f) = \sum \frac{h_j}{f^j} = \left( 10^{-18.0} + \frac{10^{-13.8}}{f} + \frac{10^{-9.9}}{f^2} + \frac{10^{-7.6}}{f^3} \right) \left( \frac{\text{volts\_ratio}^2}{\text{Hz}} \right) \Rightarrow$$

$$LdB_{xi}(f) = 10 \text{ Log } L_{xi}(f) \left( \frac{\text{dBc}}{\text{Hz}} \right)$$

Simulate  $LdB_{xi}(f)$  in *Figure 7*.

##### B. Reference Divider (frequency independent)

Phase-noise model points,  $LdB_j(f_i)$ , from fitting *General Phase Noise Model* to datasheet plot (not shown):

- Floor Segment: 0 dB/dec (3 kHz - ∞ Hz)
- Floor-point:  $LdB_0(f_a) = -153$  (3 kHz) (dBc/Hz)
- $L_0(f_a) = 10^{LdB_0/10} = 10^{-15.3}$  (3 kHz) (volts\_ratio<sup>2</sup>/Hz)
- Flicker Segment: -10 dB/dec (100 Hz - 3 kHz)
- Mid-point:  $LdB_1(f_b) = -150$  (600 Hz) (dBc/Hz)

$$L_1(f_b) = 10^{LdB_1/10} = 10^{-15.0} (600 \text{ Hz}) \text{ (volts\_ratio}^2/\text{Hz)}$$

Phase-noise model coefficients,  $h_j$ , from above phase-noise model points:

$$h_0 = L_0 f_a^0 = 10^{-15.3} \text{ (volts\_ratio}^2/\text{Hz}^{-1})$$

$$h_1 = L_1 f_b^1 = (10^{-15.0})(6(10^2))^1 = 10^{-12.2} \text{ (volts\_ratio}^2)$$

Phase-noise model,  $LdB_{ri}(f)$ , from above coefficients:

$$L_{ri}(f) = \sum \frac{h_j}{f^j} = \left( 10^{-15.3} + \frac{10^{-12.2}}{f} \right) \left( \frac{\text{volts\_ratio}^2}{\text{Hz}} \right) \Rightarrow LdB_{ri}(f) = 10 \text{ Log } L_{ri}(f) \left( \frac{\text{dBc}}{\text{Hz}} \right)$$

Simulate  $LdB_{ri}(f)$  in *Figure 7*.

##### C. Feedback Divider (frequency independent)

Phase-noise model points,  $LdB_j(f_i)$ , from fitting *General Phase Noise Model* to data sheet plot (not shown):

- Floor Segment: 0 dB/dec (10 kHz - ∞ Hz)
- Floor-point:  $LdB_0(f_a) = -155$  (10 kHz) (dBc/Hz)
- $L_0(f_a) = 10^{LdB_0/10} = 10^{-15.5}$  (10 kHz) (volts\_ratio<sup>2</sup>/Hz)
- Flicker Segment: -10 dB/dec (100 Hz - 10 kHz)
- Mid-point:  $LdB_1(f_b) = -143$  (1 kHz) (dBc/Hz)
- $L_1(f_b) = 10^{LdB_1/10} = 10^{-14.3}$  (1 kHz) (volts\_ratio<sup>2</sup>/Hz)

Phase-noise model coefficients,  $h_j$ , from above phase-noise model points:

$$h_0 = L_0 f_a^0 = 10^{-15.5} \text{ (volts\_ratio}^2/\text{Hz}^{-1})$$

$$h_1 = L_1 f_b^1 = (10^{-14.3})(10^3)^1 = 10^{-11.3} \text{ (volts\_ratio}^2)$$

Phase-noise model,  $LdB_{fi}(f)$ , from above coefficients:

$$L_{fi}(f) = \sum \frac{h_j}{f^j} = \left( 10^{-15.5} + \frac{10^{-11.3}}{f} \right) \left( \frac{\text{volts\_ratio}^2}{\text{Hz}} \right) \Rightarrow LdB_{fi}(f) = 10 \text{ Log } L_{fi}(f) \left( \frac{\text{dBc}}{\text{Hz}} \right)$$

Simulate  $LdB_{fi}(f)$  in *Figure 7*.

##### D. Prescaler (frequency independent)

Phase-noise model points,  $LdB_j(f_i)$ , from fitting *General Phase Noise Model* to datasheet plot (not shown):

- Floor Segment: 0 dB/dec (10 kHz - ∞ Hz)
- Floor-point:  $LdB_0(f_a) = -152$  (10 kHz) (dBc/Hz)
- $L_0(f_a) = 10^{LdB_0/10} = 10^{-15.2}$  (10 kHz) (volts\_ratio<sup>2</sup>/Hz)
- Flicker Segment: -10 dB/dec (100 Hz - 10 kHz)
- Mid-point:  $LdB_1(f_b) = -142$  (1 kHz) (dBc/Hz)
- $L_1(f_b) = 10^{LdB_1/10} = 10^{-14.2}$  (1 kHz) (volts\_ratio<sup>2</sup>/Hz)

Phase-noise model coefficients,  $h_j$ , from above phase-noise model points:

$$h_0 = L_0 f_a^0 = 10^{-15.2} \text{ (volts\_ratio}^2/\text{Hz}^{-1})$$

$$h_1 = L_1 f_b^1 = (10^{-14.2})(10^3)^1 = 10^{-11.2} \text{ (volts\_ratio}^2)$$

Phase-noise model,  $LdB_{pi}(f)$ , from above coefficients:

$$L_{pi}(f) = \sum \frac{h_j}{f^j} = \left( 10^{-15.2} + \frac{10^{-11.2}}{f} \right) \left( \frac{\text{volts\_ratio}^2}{\text{Hz}} \right) \Rightarrow LdB_{pi}(f) = 10 \text{ Log } L_{pi}(f) \left( \frac{\text{dBc}}{\text{Hz}} \right)$$



Simulate  $LdB_{pi}(f)$  in Figure 7.

### E. VCO (at 10 GHz scaled from 11.3 GHz given on datasheet)

Phase-noise model points,  $LdB_j(f_k)$ , from fitting *General Phase Noise Model* to datasheet plot at 11.3 GHz (not shown):

*Floor Segment:* 0 dB/dec (100 MHz -  $\infty$  Hz)  
 Floor-point:  $LdB_0(f_a) = -150(100 \text{ MHz})$  (dBc/Hz)  
 $L_0(f_a) = 10^{LdB_0/10} = 10^{-15.0}(100 \text{ MHz})$  (volts\_ratio<sup>2</sup>/Hz)  
*Flicker Segment:* -10 dB/dec (10 MHz - 100 MHz)  
 Mid-point:  $LdB_1(f_b) = -143(30 \text{ MHz})$  (dBc/Hz)  
 $L_1(f_b) = 10^{LdB_1/10} = 10^{-14.3}(30 \text{ MHz})$  (volts\_ratio<sup>2</sup>/Hz)  
*Flicker Segment:* -20 dB/dec (40 kHz - 10 MHz)  
 Mid-point:  $LdB_2(f_c) = -111(600 \text{ kHz})$  (dBc/Hz)  
 $L_2(f_c) = 10^{LdB_2/10} = 10^{-11.1}(600 \text{ kHz})$  (volts\_ratio<sup>2</sup>/Hz)  
*Flicker Segment:* -30 dB/dec (1 kHz - 40 KHz)  
 Mid-point:  $LdB_3(f_d) = -59(6 \text{ kHz})$  (dBc/Hz)  
 $L_3(f_d) = 10^{LdB_3/10} = 10^{-5.9}(6 \text{ kHz})$  (volts\_ratio<sup>2</sup>/Hz)  
*Flicker Segment:* -40 dB/dec (100 Hz - 1 kHz)  
 Mid-point:  $LdB_4(f_e) = -18(300 \text{ Hz})$  (dBc/Hz)  
 $L_4(f_e) = 10^{LdB_4/10} = 10^{-1.8}(300 \text{ kHz})$  (volts\_ratio<sup>2</sup>/Hz)

Phase-noise model coefficients,  $h_j$ , from above phase-noise model points at 11.3 GHz:

$$\begin{aligned} h_0 &= L_0 f_a^0 = 10^{-15.0} (\text{volts\_ratio}^2 \text{Hz}^{-1}) \\ h_1 &= L_1 f_b^1 = (10^{-14.3})[3(10^7)]^1 = 10^{-6.8} (\text{volts\_ratio}^2) \\ h_2 &= L_2 f_c^2 = (10^{-11.1})[6(10^5)]^2 = 10^{0.5} (\text{volts\_ratio}^2 \text{Hz}) \\ h_3 &= L_3 f_d^3 = (10^{-5.9})[6(10^3)]^3 = 10^{5.4} (\text{volts\_ratio}^2 \text{Hz}^2) \\ h_4 &= L_4 f_e^4 = (10^{-1.8})[3(10^2)]^4 = 10^{8.1} (\text{volts\_ratio}^2 \text{Hz}^3) \end{aligned}$$

Phase-noise model,  $LdB_{vi}(f)$ , from above coefficients [ $L_{11.3}(f)$  at 11.3 GHz given on datasheet scaled to  $L_{vi}(f)$  at 10 GHz]:

$$\begin{aligned} L_{11.3}(f) &= \sum \frac{h_j}{f^j} = \left(10^{-15.0} + \frac{10^{6.8}}{f} + \frac{10^{0.5}}{f^2} + \frac{10^{5.4}}{f^3} + \frac{10^{8.1}}{f^4}\right) \left(\frac{\text{volts\_ratio}^2}{\text{Hz}}\right), \\ L_{vi}(f) &= \left(\frac{10}{11.3}\right)^2 L_{11.3}(f) \left(\frac{\text{volts\_ratio}^2}{\text{Hz}}\right) \Rightarrow LdB_{vi}(f) = 10 \text{ Log } L_{vi}(f) \left(\frac{\text{dBc}}{\text{Hz}}\right) \end{aligned}$$

Simulate  $LdB_{vi}(f)$  in Figure 7.

### F. Phase Detector (at 25 MHz)

Phase-noise model points,  $LdB_j(f_k)$ , from fitting *General Phase Noise Model* to datasheet plot (not shown):

*Floor Segment:* 0 dB/dec (1 kHz -  $\infty$  Hz)  
 Floor-point:  $LdB_0(f_a) = -159(1 \text{ kHz})$  (dBc/Hz)  
 $L_0(f_a) = 10^{LdB_0/10} = 10^{-15.9}(1 \text{ kHz})$  (volts\_ratio<sup>2</sup>/Hz)  
*Flicker Segment:* -10 dB/dec (100 Hz - 1 kHz)  
 Mid-point:  $LdB_1(f_b) = -154(300 \text{ Hz})$  (dBc/Hz)  
 $L_1(f_b) = 10^{LdB_1/10} = 10^{-15.4}(300 \text{ kHz})$  (volts\_ratio<sup>2</sup>/Hz)

Phase-noise model coefficients,  $h_j$ , from above phase-noise model points:

$$\begin{aligned} h_0 &= L_0 f_a^0 = 10^{-15.9} (\text{volts\_ratio}^2 \text{Hz}^{-1}) \\ h_1 &= L_1 f_b^1 = (10^{-15.4})[3(10^2)]^1 = 10^{-12.9} (\text{volts\_ratio}^2) \end{aligned}$$

Phase-noise model,  $LdB_{di}(f)$ , from above coefficients:

$$L_{di}(f) = \sum \frac{h_j}{f^j} = \left(10^{-15.9} + \frac{10^{-12.9}}{f}\right) \left(\frac{\text{volts\_ratio}^2}{\text{Hz}}\right) \Rightarrow LdB_{di}(f) = 10 \text{ Log } L_{di}(f) \left(\frac{\text{dBc}}{\text{Hz}}\right)$$

Simulate  $LdB_{di}(f)$  in Figure 7.

### G. Loop Filter/Error Amplifier (frequency N/A)

Not modeled, as mentioned, since it's not an RF component with intrinsic phase noise. Modeling its *effective* phase noise, as well as calculating its propagation dynamics that contribute to output phase noise, is more complex than for an RF component.<sup>1</sup>

## 5. Determine the loop bandwidth, $f_g$ , from the sole specification of the lowest average output phase noise across the band by achieving the lowest phase noise at the 10-GHz mid-band output.

The loop optimum bandwidth,  $f_g$ , is determined from the intersection of the VCO and pedestal (see definition below) phase-noise curves at the 10-GHz mid-band output.

VCO phase noise model at 10 GHz,  $LdB_{vi}(f)$ , and curve is as is in the aforementioned section 4, part E.

Pedestal phase-noise model at 10 GHz,  $LdB_{pi}(f)$ , and curve, where the pedestal is defined as the sum of all RF components' (except the VCO) phase-noise models,  $L_{si}(f)$ , multiplied by the output transfer function's (to be discussed later) dc gain squared,  $N^2$ :

$$\begin{aligned} L_{si}(f) &= \frac{L_{si}(f)}{R^2} + L_{vi}(f) + L_{ri}(f) + L_{pi}(f) + L_{di}(f) \text{ with } R = 4 \left(\frac{\text{volts\_ratio}^2}{\text{Hz}}\right), \\ L_{pi}(f) &= L_{si}(f)N^2 \left(\frac{\text{volts\_ratio}^2}{\text{Hz}}\right) \Rightarrow LdB_{pi}(f) = 10 \text{ Log } L_{pi}(f) \text{ with } N = 400 \left(\frac{\text{dBc}}{\text{Hz}}\right) \end{aligned}$$

Simulate  $LdB_{pi}(f)$  in Figure 7.

The loop bandwidth is then determined either mathematically or graphically and is found to be  $f_g = 121.6 \text{ kHz}$ .

## 6. Determine the standard parameters $f_n$ and $\zeta$ .

We determine  $f_n$  by using rule-of-thumb  $f_n = f_g / 1.55$  for  $\zeta = 0.707$  (*Reference 2*) and we determine  $\zeta$  from other specifications (other specifications not given so  $\zeta = 0.707$  is retained as default). These were found to be:

$$\begin{aligned} f_n &= 78.5 \text{ kHz} \\ \zeta &= 0.707 \end{aligned}$$

## 7. Equate the open-loop transfer function, $T_{ol}$ , 2nd order form (bold) to the circuit constant form (bold), which gives standard parameters $f_n$ and $\zeta$ in terms of circuit constants $R_1$ , $R_2$ , and $C_1$ .

(convert to  $\omega_n = 2\pi f_n$ )

$$\begin{aligned} T_{ol}(s) &= \frac{2\zeta\omega_n}{s} + \frac{\omega_n^2}{s^2} = K_\phi F(s)K_o K_n = \frac{K_\phi F(s)K_v}{sN} \\ \frac{K_\phi \left(\frac{s\tau_2+1}{s\tau_1}\right)K_v}{sN} &= \frac{(K_\phi K_v R_2 C_1)/(NR_1 C_1)}{s} + \frac{(K_\phi K_v)/(NR_1 C_1)}{s^2} (\text{volts\_ratio}) \end{aligned}$$

which gives the desired relations (bold):

$$\omega_n = \sqrt{\frac{K_\phi K_V}{N\tau_1}} = \sqrt{\frac{K_\phi K_V}{NR_1 C_1}} \quad \left(\frac{\text{rad}}{\text{sec}}\right),$$

$$\zeta = \frac{\omega_n \tau_2}{2} = \frac{\omega_n R_2 C_1}{2} = \frac{\tau_2}{2} \sqrt{\frac{K_\phi K_V}{N\tau_1}} = \frac{R_2}{2} \sqrt{\frac{K_\phi K_V C_1}{NR_1}}$$

**8. Determine circuit constants  $R_1$ ,  $R_2$ , and  $C_1$  (bold) as functions of standard parameters  $f_n$  and  $\zeta$  for the 10-GHz mid-band output ( $N = 400$ ) and calculate any other quantities of interest; modify theoretical values to closest EIA 5% standard values.**

$$\tau_1 = \frac{K_\phi K_V}{\omega_n^2 N} \quad (\text{sec}),$$

$$\tau_2 = \frac{2\zeta}{\omega_n} = 2\zeta \sqrt{\frac{NR_1}{K_\phi K_V}} \quad (\text{sec}),$$

$$R_1 = \frac{K_\phi K_V}{\omega_n^2 N C_1} \quad (\Omega),$$

$$R_2 = \frac{2\zeta}{\omega_n C_1} = 2\zeta \sqrt{\frac{NR_1}{K_\phi K_V C_1}} \quad (\Omega),$$

$$C_1 = \frac{K_\phi K_V}{\omega_n^2 N R_1} \quad (\text{F})$$

(convert back to  $f_n = \omega_n/2\pi$ ).

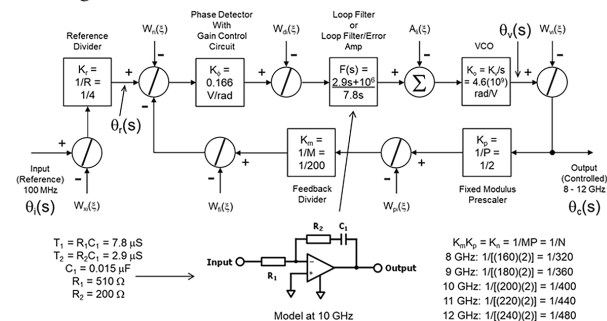
Note that  $R_1$ ,  $R_2$ , and  $C_1$  are not uniquely determined, so an absolute selection must be made for one of them, usually  $C_1$ . For this case, select  $C_1$ , then calculate  $R_1$  and  $R_2$  (all for resonant frequency of  $f_n = 78.5$  kHz and damping factor of  $\zeta = 0.707$ ), where  $C_1$  is selected to keep  $R_1$  and  $R_2$  relatively low. Therefore, resistive noise is insignificant relative to error amplifier (op amp) noise, and within practical limits:<sup>12,13</sup>

$$C_1 = 0.015 \mu\text{F} \text{ (already 5\% standard value)}$$

$$R_1 = 522.9 \Omega \text{ (5\% standard value is } 510 \Omega)$$

$$R_2 = 191.1 \Omega \text{ (5\% standard value is } 200 \Omega)$$

Using these standard values, the design is done and the system is configured by applying the *General PLL Block Diagram and Phase Noise Propagation Model* (Fig. 4, Part 1) to our specific case to form the *Specific PLL Block Diagram & Phase Noise Propagation Model at 10 GHz Mid-band Output for Example PLL* (Fig. 8).<sup>14</sup>



8. Specific PLL Block Diagram & Phase Noise Propagation Model at 10-GHz mid-band output for 8- to 12-GHz output/50-MHz step PLL frequency synthesizer.

**9. Model PLL open-/closed-loop dynamics and output phase noise, and simulate performance using appropriate modeling/simulation tool.**

Adjust model theoretical (standard value) circuit constants and open-loop gain as needed for closest agreement between simulated and calculated loop dynamics, as well as output phase noise due to discrepancies between calculated and simulated performance.

**10. Build and test EDM unit.**

Using adjusted circuit constants, build and test the EDM unit. Further adjust EDM circuit constants as needed for proper performance due to discrepancies between simulated and EDM performance.

**11. Adjust model open-loop gain as needed for agreement between the model and EDM unit.**

So, the design is complete using the theoretical (standard value) circuit constants as determined in step 8. These values would then be refined according to steps 9, 10, and 11, but since we’re not building an EDM for our example, the theoretical values complete the design.

The above information is used in the final Part 3, where we analyze our example hypothetical synthesizer to demonstrate the concepts and methods presented. ■

**REFERENCES**

1. F. M. Gardner, "Phaselock Techniques", 3<sup>rd</sup> ed., John Wiley, Hoboken, NJ, 2005.
2. R. E. Best, "Phase-Locked Loops, Design, Simulation and Applications", 6<sup>th</sup> ed., McGraw-Hill, New York, NY, 2007.
3. P. V. Brennan, "Phase-Locked Loops: Principles and Practice", McGraw-Hill, New York, NY, 1996.
4. E. Drucker, "Phase Lock Loops and Frequency Synthesis for Wireless Engineers", 1997, Frequency Synthesis & Phase-Locked Loop Design, 3 Day Short Course, Besser Associates, Mountain View, CA, 1999.
5. F. C. Weist, "Phase Locked Loop Basics for Frequency Synthesizer Applications", Short Course, Clarksburg, MD, 2011.
6. P. Z. Peebles, Jr., "Probability, Random Variables and Random Signal Principles", McGraw-Hill, New York, NY, 1980.
7. A. Godone, S. Micalizio and F. Levi, "RF spectrum of a carrier with a random phase modulation of arbitrary slope", Istituto Nazionale di Ricerca Metrologica, INRIM, Strada delle Cacce 91, 10135 Torino, Italy, Metrologia, vol. 45, pp. 313-324, BIPM and IOP Publishing Ltd., Bristol BS1 6HG, UK, May 2008.
8. B. Nelson, "Phase noise 101: basics, applications and measurements", Keysight Technologies, 2018.
9. A. El Gamal, EE278 Lecture Notes 7: "Stationary random processes", Dept. of Electrical Engineering, College of Engineering, Stanford University, Stanford, CA, Autumn 2015.
10. K. J. Button, ed., Infrared and Millimeter Waves, Volume 11: Millimeter Components and Techniques, Part III, Chapter 7: "Phase Noise and AM Noise Measurements in the Frequency Domain", A. L. Lance, W. D. Seal and F. Labaar, TRW Operations and Support Group, One Space Park, Redondo Beach, CA, Academic Press, Cambridge, MA, 1984.
11. Harney, A., "Designing high-performance phase-locked loops with high-voltage VCOs", Analog Dialogue, pp. 43-12, December 2009.
12. "Op amps for everyone", Design Reference, Literature Number SL00006A, Texas Instruments Inc., Dallas, Texas, 2001.
13. "Noise analysis in operational amplifier circuits", Application Report, Literature Number SLVA043B, Texas Instruments Inc., Dallas, Texas, 2007.
14. Motorola Communications Device Data, Data Book, DL136/D, REV 4, Phoenix, AZ, 1995.



### E-Band WR12 Waveguide Passive Components Serve Challenging Systems

Smiths Interconnect is extending its range of passive components in E-band with the addition of WR12 coupler, loads and isolators, designed for next-generation E-Band terrestrial uplinks to LEO constellations and payloads. Each product has been optimized to sustain a robust communications link for any application, even if it has specific environmental demands. The E-band WR12 waveguide hybrids offer tuneless and broadband performance suitable for global applications as well as signal-splitting and combining applications.

**SMITHS INTERCONNECT**

<https://tinyurl.com/yps88sh9>

### RF Balun Transformer Tackles 10 to 24 GHz

Mini-Circuits' model MTY2-243+ is a balanced/unbalanced (balun) RF transformer with a 2:1 impedance ratio from 10 to 24 GHz. It exhibits typical insertion loss of 1.0 to 1.5 dB. Amplitude unbalance is typically 0.7 dB while phase unbalance is typically 6°. Fabricated with a proven HBT process, the 50-Ω MMIC RF transformer measures just 2 × 2 × 1 mm but handles as much as +31 dBm input power. It is a good fit for radar, satellite communications, and instrumentation.

**MINI-CIRCUITS**

<https://tinyurl.com/ypmngsqf>



### Low-Noise Amplifier Boosts 71 to 86 GHz

Mini-Circuits' model WVA-71863LNX+ is a low-noise amplifier (LNA) with 39-dB typical gain from 71 to 86 GHz. It maintains gain within ±1.5 dB across its bandwidth and holds noise figure to typically 5 dB or less. Well suited for aerospace/defense systems, radar, and test applications, the LNA delivers +14.5 dBm typical output power at 1-dB compression and runs from supply voltages from +10 to +15 VDC. It incorporates over-voltage and reverse-voltage protection and is equipped with WR12 interfaces.

**MINI-CIRCUITS**

<https://tinyurl.com/yuj9odaz>



### Flexible PXI/PXIe Microwave Switches Address Performance & Test System Optimization

Pickering Interfaces released the 40/42-890 family of modular, flexible PXI/PXIe microwave switches, bringing highly configurable RF switching solutions up to 110 GHz to the PXI platform. Supporting

the latest and most demanding RF and communications test requirements as operating frequencies continue to evolve to ever higher levels, the new 40/42-890 microwave switch family provides highly configurable RF switching solutions via the PXI platform.

**PICKERING INTERFACES**

<https://tinyurl.com/2xxjwatx>

### G-Type Mounts for Horn Antennas Enhance Setup and System Performance

Fairview Microwave introduced G-type (round) mounts for standard-gain horn antennas, with the capability to significantly improve the setup process for test and measurement purposes. The

G-type round mounts accommodate a broad spectrum of waveguide sizes, with 19 variants that address waveguide sizes ranging from WR28 to WR2300, and their respective IEC counterparts. The aluminum mounts have a durable interior finish of chromate conversion complemented by an anticorrosion gray paint exterior to ensure longevity while adding to the functionality of the entire system. The cage-style design simplifies the antenna attachment process, thereby enhancing the stability of the entire setup.



**FAIRVIEW MICROWAVE**

<https://tinyurl.com/ykbsw9z5>

# FUTURE DIRECTIONS FOR LPWANs AND THE IOT/IOT

## LEARN MORE IN OUR FREE ON DEMAND WEBINAR CREATED BY MICROWAVES & RF

LPWANs are the backbone that connects a multitude of battery-powered IoT/IoT devices in applications such as asset tracking, occupancy detection, smart metering, and many others. There are several factors that wireless-network designers and integrators will want to consider as they sort through the various technologies available to them:

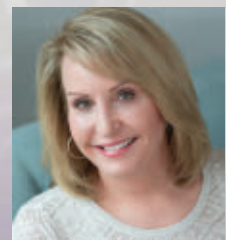
- What's the current state of the IoT/IoT landscape? What is driving IoT adoption?
- How will LPWAN augment and work with other technologies like Wi-Fi and Bluetooth?
- What are some of the emerging applications for LPWANs?
- How will LPWANs address challenges of scalability?
- How will organizations like the LoRa Alliance continue making it easier to implement, develop, and deploy LPWANs?

**REGISTER NOW AT:**

<http://www.mwrf.com/21265303>



Speakers:



*Donna Moore,  
CEO and Chair of the  
LoRa Alliance*